Jean-Marc Guarini, Gérard Blanchard and Pierre Richard

Modelling the dynamics of the microphytobenthic biomass and primary production in European intertidal mudflats

Abstract

A mathematical model was formulated in order to simulate the local dynamics of the microphytobenthic biomass of an intertidal mudflat community. The model was based on three sets of processes that drive the dynamics of the system. First, the intertidal benthic microalgae are able to migrate quickly to the mud surface to constitute a dense biofilm at the beginning of the daytime emersion period. At the end of the daytime emersion period, the microphytobenthos burrows into the aphotic layer of the mud and the biofilm disappears completely. Secondly, photosynthetic primary production occurs in the biofilm at the mud surface during the daytime emersion period, and production mainly depends on light and temperature forcing variables. And finally, the third set represents any losses of biomass that affect the dynamics slowly; this set of processes encompasses stress-induced mortality, grazing and resuspension of microphytobenthos into the water column during submersion periods. At the ecosystem level, primary production is controlled mainly by physical synchronizers (tidal and light-dark cycles).

The mathematical properties of the initial model were characterized by a stable steady state and a short resilience time. The underlying concepts of the formulation were tested with comparisons between simulations and observations and the model description was consistent with the observed patterns of biomass dynamics. Nevertheless, two groups of processes were not sufficiently well-described: vertical migration of the microphytobenthos and biomass loss. The losses were too poorly constrained; the grazing losses could not be distinguished from resuspension. The stimuli for vertical migration were also not fully understood and only an integrated vertical migration was taken into account. In particular, the trigger for the downward vertical migration, at the end of a daytime emersion period, is unknown and remains controversial.

Therefore, the model was reformulated with some new hypotheses linking the rhythms of vertical migrations to resuspension into the water column. New experiments were designed, mainly to characterize the biofilm and its ability to produce new biomass. Additional studies of the mathematical properties of the model provided new perspectives for validation and future work. This approach is the first step in proposing an integrated theory for the dynamics of the pelagic and

Functioning of microphytobenthos in estuaries.
Royal Netherlands Academy of Arts and Sciences, 2006

benthic microalgal biomass and primary production in European-type semi-enclosed littoral ecosystems. Testing the validity of this integrated theory will require accurate quantification of biomass exchanges between the benthic and pelagic compartments.

Introduction

One of the main challenges in ecology is making accurate estimates of the productivity of marine ecosystems. This is particularly critical when ecosystems are exploited for their renewable resources. Semi-Enclosed Littoral Ecosystems (SELE including bays, lagoons, estuaries and deltas) are highly productive (Schelske and Odum 1962; Walker and Mossa 1982). Several types of SELE which generate large amounts of organic matter can be defined and in particular, McLusky (1989) has ranked SELE between two endpoints based on their primary producers. At one end of the McLusky classification scheme were American-Type SELE. These ATSELE are characterized by salt marshes with halophytes that provide a large amount of detritic organic matter through decomposition of the plant material. A part of the detritic biomass is used by the benthic and pelagic foodwebs, and the remaining fraction is exported to the open coastal zone (Long and Mason 1983; Wetzel and Sin 1998). At the opposite end, McLusky placed European-Type SELE, which are characterized by wide, bare intertidal mudflats without any macrophytic primary production. The high primary productivity in these ETSELE is supported mainly by microalgal communities that colonize both the water column and the sediments (Admiraal 1984; McLusky 1989; Underwood and Kromkamp 2000). This type of ecosystem is widely distributed along the European coastline, and building a quantitative description of the dynamics of these ecosystems is of fundamental importance to the understanding and management of the coastal resources of Europe (Figure 1).

The quantification of phytoplankton production in shallow water ecosystems (see Cloern 1996 for a review) is more advanced than the quantification of the dynamics of microphytobenthos living on intertidal mudflats. However, there is no existing general theory which describes the dynamics of phytoplankton in shallow-water ecosystems (Lucas *et al*. 1998). Theories developed for open oceanic areas cannot be applied because of the short-term variability and the absence of persistent stratification in shallow water tidal ecosystems (Pritchard 1967; Legendre 1981). In addition, both the benthic and pelagic microalgal compartments are tightly linked in ETSELE (Shaffer and Sullivan 1988). This linkage between the microphytobenthos and phytoplankton suggests that a part of the biomass observed in the water column is due to the resuspension of the benthic microalgae from the mudflat (Demers *et al*. 1987; de Jonge and van Beusekom 1992; 1995; Lucas *et al*. 2001). The resuspended fraction is important but has been difficult to determine accurately because it fluctuates as a function of both the hydrodynamic conditions and the microphytobenthic biomass in the surficial layer of the sediment. Thus the resuspension dynamics of the microphytobenthic biomass cannot be quantified as long as the dynamics of the microphytobenthic biomass itself remains unknown at the scale of the ecosystem.

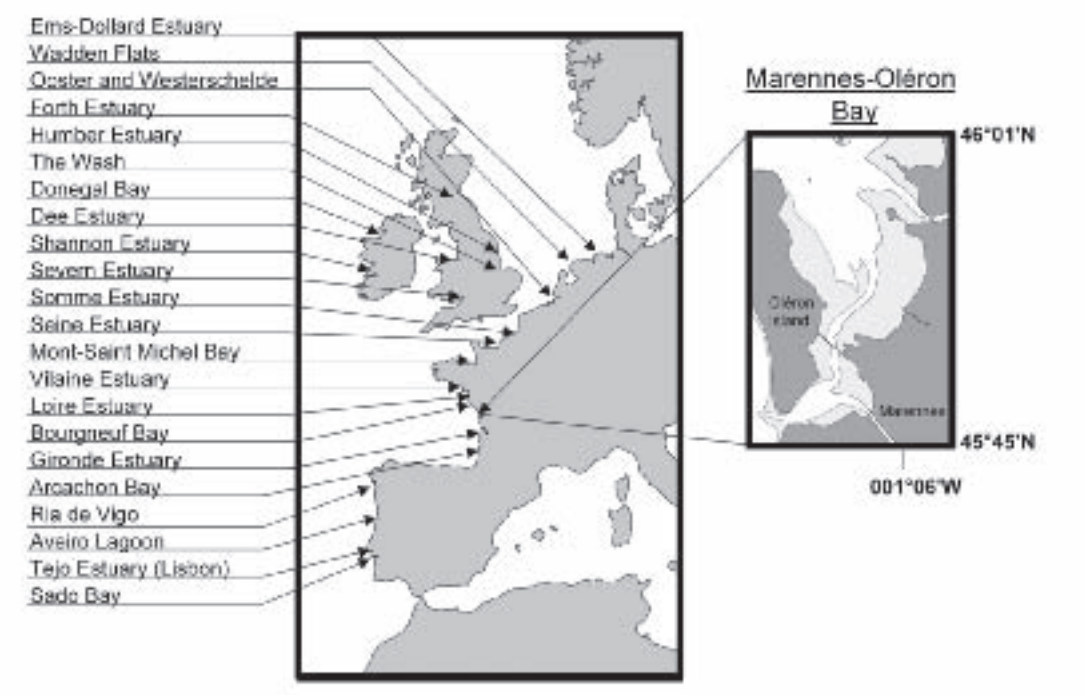

Figure 1. European-Type Semi-Enclosed Littoral Ecosystems (ETSELE) along the European coast. They are characterized by a high tidal range and wide, bare intertidal flats sustaining an important microphytobenthic production. The Marennes-Oléron Bay belongs to this category of ecosystems (60% of the total area are intertidal flats), and is one of the major sites for shellfish cultures in France.

Much conceptual progress has been made in characterizing intertidal microphytobenthos and its dynamics, mostly with respect to three areas: active vertical migration, the formation of the microphytobenthic biofilm during daytime emersion periods (Paterson *et al*. 1998; Serodio et Catarino 2000; Guarini *et al*. 2000a), and benthic primary production (Underwood and Kromkamp 2000). Important differences exist between the pelagic and the benthic systems of primary production. In particular, the way in which the microphytobenthos concentrates in the surficial layers of sediment and their active movement to reach the surface of the mud (Hay *et al*. 1993) contrast with the conditions in a well-mixed water column, in which the phytoplankton is transported passively and is exposed periodically to a variable light energy as a function of the vertical mixing intensity (Marra 1978; Legendre 1981). These differences require a new scheme to represent the dynamics of the microphytobenthos, and new techniques to study the processes over appropriate time intervals. Among them are separation techniques that exploit the active vertical migration of pennate diatoms (Couch 1989), and micro-scale techniques to measure the photosynthetic activity of the biofilm such as O_2 microelectrodes and Pulse Amplitude Modulated fluorimetry (Serôdio and Catarino 2000).

Quantification of the microphytobenthos resuspension remains difficult to estimate. The resuspension of the microphytobenthos is generally attributed to erosion processes induced by currents – mostly those generated by tidal oscillations – and waves (Demers *et al*. 1987; de Jonge and van Beusekom 1995). Therefore, in order to quantify the resuspension of the microalgal biomass, biological processes of production must be coupled with sedimentary processes of mud erosion. This coupled approach has been difficult to achieve because the results of hydro-sedimentary models are very sensitive to the critical shear-stress of the mud (McDonald and Cheng 1997) and the vertical distribution of the microphytobenthic biomass in the surficial layers of the mud is not well-known. This vertical distribution changes over time and the uncertainty in the thickness of the eroded layer of particles has the same order of magnitude as the thickness of the layer that contains the photosynthetically active biomass. Therefore, the entire photosynthetically active biomass can be resuspended all at once when this type of model is used. The fundamental question of population survival must be considered if the entire superficial layer is constantly eroded at each flood tide.

The objectives of this chapter are to review the processes that govern the biomass dynamics of the microphytobenthos inhabiting intertidal mudflats and to discuss how these processes can be evaluated and tested within a common conceptual framework by both experimental and mathematical (modelling) studies. A mathematical model specifically designed to quantify the dynamics of the biomass at the level of an ETSELE is proposed. This model is minimal; it only takes into account the main processes that govern the biomass dynamics, and the processes that are not well-known are represented by the simplest formulation possible (i.e. a linear function of the microphytobenthic biomass is used). The processes included in the proposed model are: the vertical migration, the primary production, the losses by grazing and stress-induced mortality, and the resuspension and transport of the biomass. Finally, the validation of the model is discussed using the first elements of a comparison between simulations and observations of a quantified benthic-pelagic coupling for the microalgal biomass.

Scales of variations and the conceptual scheme

Quantification of the intertidal microphytobenthos dynamics over an entire ecosystem requires a description that can include four spatial scales (microscale, mesoscale, macroscale and regional scale) each of which is associated with a deterministic component of the system. The microscale (between 1 μm and 1 cm) is the scale of the microalgae and is associated with the structure of the system. Electron microscope observations have shown that the formation of the microalgal biofilm at the mud surface during the daytime emersion period (Paterson 1989) and this biofilm (Figure 2) is a thin layer of contiguous cells which covers the surface of the mud. The mesoscale (between 1 cm and 1 meter) is an intermediary scale. It is the scale of the microphytobenthos patchiness, which varies as a function of the production and biomass (Seuront and Spilmont 2002; Saburova *et al*. 1995). The macroscale (between 1 m and 1 km) is associated with the geomorphological support of the system, and changes seasonally as a function of sedimentary processes (sedimentation, erosion or compaction events, Le Hir *et al*.

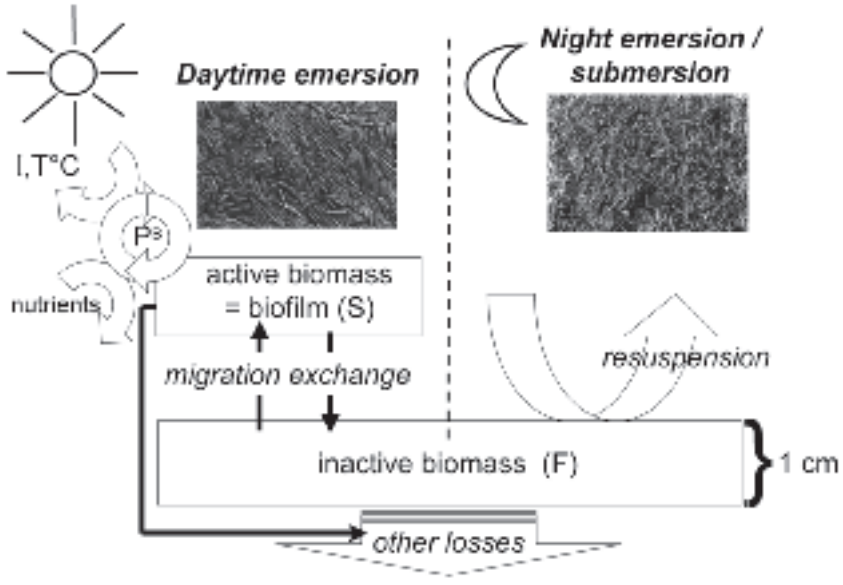

Figure 2. Conceptual scheme to describe the dynamics of the microphytobenthic biomass intertidal mudflat. The classical scheme of a unique compartment with a biomass distributed in a vertical gradient of light is replaced by a scheme of two discrete compartments, introducing a microalgal biofilm at the mud surface where the biomass (S) is concentrated and a reservoir where the biomass (F) is diluted into the first centimetre of the mud. The biofilm is a temporary structure that exchanges biomass with the reservoir compartment during daytime emersion only. The biofilm disappears during night emersion and submersion periods. Resuspension occurs only during immersion while losses by grazing or natural mortality affect the overall biomass at all times.

2000). At macroscale, the presence of the biofilm can be observed by a color change at the surface of consolidated muds; areas of unconsolidated mud, such as in runnels, do not develop a microalgal biofilm. Thus at the macroscale, the distribution of available mud surface for biofilm development must be considered. The regional scale (between 1 km and 100 km) is the scale of the tidal ecosystem. It is associated with the concept of habitats and intertidal subtidal areas must be delimited. At this scale, long-term changes affect the coastline and the bathymetry of the ecosystem.

The model design integrated the variability at mesoscale and represented the averaged dynamics of the microalgal biomass in a standard square meter of the mud surface. In the chapter devoted to the observation of the local dynamics of the biomass (Blanchard *et al*. this book), the sampling procedure used in the field studies was designed to be consistent with the modelling approach, and the size of the sampling unit was chosen to minimize mesoscale variability.

The mathematical model simulates the dynamics of the intertidal mudflat microphytobenthos at macroscale, based on the concepts and assumptions that come from the observations and experiments realized at microscale. The mathematical behaviour

of the model was studied in order to characterise the properties of the microphytobenthos dynamics at the regional scale. The persistence of the benthic biomass is characterised by studying the steady state conditions of the simulations. The convergence to steady state conditions, representing the resilience of the system, describes how the benthic biomass responds to disturbances (*e.g.* suspension and sedimentation). Global trends are addressed by examining long-term changes of the steady state reached in the simulations.

At macroscale, horizontal movements of the diatoms can be neglected, and a local model (built with ordinary differential equations) that does not take into account spatial variations can be formulated, representing the dynamics of the benthic biomass in one square meter of mudflat. The square-meter of consolidated mud is assumed to be homogeneous and emerged at least once per neap-to-spring tide cycle. Inside this ideal square-meter takes place – potentially – the vertical migration and the formation of the biofilm during a daytime emersion period.

Only the biomass in the first centimetre of the mud is considered potentially active for photosynthesis and it is a part of this biomass that migrates up to the surface during a daytime emersion period to create the biofilm on the mud surface. The depth of light penetration is so shallow (not more than few hundred microns) that it can be neglected in the calculations. The light penetration depth is small compared to the micro-topography of the mud surface and has the same order of magnitude as the diatoms themselves. In addition, the layer of cells at the surface are so densely packed that they reduce the light penetration by self-shading, and therefore, it is assumed that only the microalgal biomass in the biofilm can produce and benefit from all the incident light energy available at the surface. This primary production and the vertical migration of the cells are controlled by the combination of the tidal and the light-dark cycles, which are considered to be deterministic.

This conceptual description (Figure 2) and approach differs considerably from previous modelling attempts (Pinckney and Zingmark 1993; Serôdio et Catarino 2000) since the representation of a partially active biomass as a continuous mass gradient that migrates in a light gradient (Pinckney and Zingmark 1991), is replaced with a biofilm which is a discrete, temporary and renewable structure, that ensures both production and growth of the community during daytime emersion periods. The biofilm is thus a functional structure created by the microalgal community that has migrated from the aphotic uppermost centimetre of the mud and also a structure that disappears near the beginning of the submersion period, or under a light threshold, when the microalgal cells either bury themselves into the sediment or become resuspended into the water column.

Modelling the local dynamics of the microphytobenthos

Microphytobenthic biofilm and active vertical migration

The modelling approach is based on the two main components of the conceptual description: the biofilm and the active vertical migration of the microphytobenthos.

The net vertical migration rhythm has been studied and described by many authors (Palmer and Round 1965; 1967, Hay *et al*. 1993; Serôdio *et al*. 1997) and a formal quantification is proposed here. Two state variables were defined: S, which represents the concentration of chlorophyll *a* per square meter in the biofilm on the mud surface (S in (mg Chl *a*) m^{-2}), and F which represents the concentration of chlorophyll *a* per square meter in a layer of mud one centimetre thick (F in the uppermost centimetre, in (mg Chl *a*) m^{-2}).

At the start of a daytime emersion period, the net vertical migration is oriented upwards and a dense layer of cells progressively covers the mud surface until all available space is occupied (Figure 2 and 3). Thus, the net upward migration process can be considered a density-dependant process that stops when space becomes limited, even if individual cells are renewed, without being detected. The surface space remains "saturated" with respect to diatom cells as long as the biofilm can be renewed, and within the limits of the daytime emersion period.

The following three sets of differential equations (Equations 1a, 1b, 1c) describe the dynamics of the exchanges between the aphotic layer of sediment (the uppermost

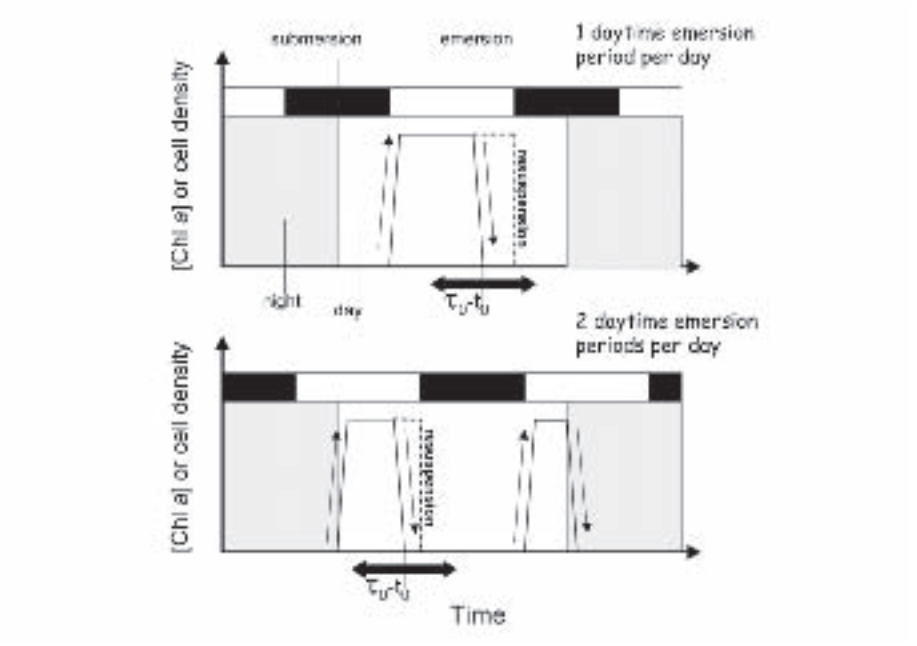

Figure 3. Conceptual scheme to describe the vertical migration in the context of the dynamics of the microphytobenthic biomass. The active vertical migration allows exchanges between S and F to occur. At the beginning of each daytime emersion period, the chlorophyll a concentration (the number of cells) increases rapidly at the surface to constitute the biofilm. The net vertical migration stopped when all the available space is occupied at the mud surface. The biofilm disappears completely at the end of the daytime emersion period, when the microalgae burrow into the sediment or if the biofilm is resuspended into the water column.

centimetre of the mud containing the biomass F) and the biofilm which contains the biomass, S. S and F have initial values equal to S_0 and F_0 respectively. A third variable, τ, is introduced to represent the time spent by the biofilm at the mud surface during a daytime emersion period. This time is set at the beginning of the daytime emersion by the initial condition, τ_0.

During daytime emersion periods:

If $\tau > 0$ If $\tau \leqslant 0$ [1a]

$$\begin{cases} \frac{dS}{dt} = + r_F F (1 - S/S_{max}) \\ \frac{dF}{dt} = - r_F F (1 - S/S_{max}) \\ \frac{d\tau}{dt} = - 1 \end{cases} \qquad \begin{cases} \frac{dS}{dt} = - r_S S \\ \frac{dF}{dt} = + r_S S \\ \frac{d\tau}{dt} = - 1 \end{cases}$$

The time, τ, controls net exchanges. As long as τ is positive, a part of F is transferred into S until the saturation value of the biomass in the biofilm (S_{max}) is reached. The transfer rate is: r_F (T^{-1}). When S is equal to S_{max}, net exchanges stop, and when τ becomes null or negative, even if the daytime emersion period is not finished, net exchanges are reversed; S is transferred into F, with a transfer rate of r_S (T^{-1}), until the biofilm disappears completely.

The initial condition, τ_0, can be determined according to several different hypotheses. The initial condition can coincide with the duration of the daytime emersion, assuming that pennate diatoms can anticipate (under internal or external factors) a submersion period and bury themselves into the mud before the flooding tide arrives. It could also be regulated by an internal rhythm that takes into account the combination of the tidal and the light cycles, including the phase difference between the synchronizers. This second hypothesis is slightly different from the first one, because the diatoms anticipate the flood, unless environmental conditions (changes in atmospheric pressure, wind speed or direction) modify its timing. For the third hypothesis, the initial condition is determined by the community itself, and depends on the total biomass in the first centimetre of the mud. In this case, τ_0 can be described by a function, f, of the total biomass (F_0+S_0) and S_{max}:

$$\tau_0 = f\left(\frac{F_0 + S_0}{S_{max}}\right)$$

The net migration behaviour during night emersion periods can be described as:

$$\begin{cases} \frac{dS}{dt} = - r_S S \\ \frac{dF}{dt} = + r_S S \\ \tau = \tau_0 \end{cases} \qquad [1b]$$

Under a light threshold, cells migrate downward into the sediment, and the chlorophyll *a* concentration S is transferred to F with the rate r_S (T^{-1}). Then, τ is set to its initial value, τ_0, for the next daytime emersion period.

During submersion periods, no vertical migration occurs and the system is described by:

$$\begin{cases} S = 0 \\ \frac{dF}{dt} = 0 \\ \tau = \tau_0 \end{cases} \qquad [1c]$$

No exchange occurs between S and F during a submersion period. The transition period between emersion and submersion is considered to be instantaneous at the scale of this dynamic. A fraction of the microphytobenthic biomass, S, is swept away by the flooding tide waters if the cells have not migrated down into the sediment before the end of the daytime emersion period. Afterwards, as in the night emersion period, τ is set to its initial value, τ_0, for the next daytime emersion period.

Simulations of this first model of vertical migration are performed by the commutation between the three systems [Equations 1a, 1b, 1c], and using the three hypotheses formulated about the variable τ (Figure 3). Figure 3A shows the results using the hypothesis of a complete synchronization between the vertical migration rhythm and the daytime emersion period. At the beginning, the biofilm is formed at the mud surface; S increases from 0 to S_{max}, and F decreases from F_0 to (F_0-S_{max})). Just before the end, the biofilm disappears, S decreases from S_{max} to 0, and F increases from (F_0-S_{max}) to F_0. No resuspension occurred for any initial conditions. Figure 3B corresponds to the second hypothesis. In this case, the vertical migration rhythm is fixed and cannot change. Therefore, if the flood is anticipated, S (which is equal to S_{max}) is resuspended in the water column, and the total biomass (F+S) decreased from any initial conditions (F_0+S_0), to reach zero, eventually.

The results from simulations based on the third hypothesis are shown in Figure 3C. The duration of the biofilm at the mud surface is a function of the initial biomass at the beginning of the daytime emersion period. A critical biomass B_c, above which the biofilm is resuspended in the water column, was defined and depends on the saturation value of the biofilm S_{max}, on the average duration spent by a unit of biomass (corresponding to S_{max}) at the mud surface, τ_s, and on the duration of the day-time emersion period, T_E:

$$B_c = S_{max} \frac{T_E}{\tau_s}$$

Under these conditions, the biomass F tended to decrease below the critical value of B_c such that no resuspension occurred.

Resuspension of the microphytobenthos always affects the value S (the biofilm) and occurred most of the time when S was equal to S_{max}. These simulations described the dynamics of the microphytobenthic biomass in the absence of production, grazing, mortality, and sediment erosion events that could induce the resuspension of a

fraction of F. The situation becomes more complex if a neap to spring tide cycle is superimposed on the tidal cycle. In this case, two daytime emersion periods can occur per day with shorter durations (Figure 4). The daytime emersion period can be followed by a night emersion during which no resuspension occurs because the biofilm disappears when the incident light is under the threshold level, in other words the diatoms have buried themselves into the sediment.

Introducing local production and loss processes.

The dynamics of the biomass are governed by the production and loss processes and added to the system of differential equations that describes the net vertical migration behaviour of the microphytobenthic community. Loss processes include stress-induced mortality and benthic grazing by surface deposit feeders (thus decreasing S) and subsurface deposit feeders (decreasing F). For the compartment F, the loss terms can also represent any of several possible processes that bury cells in deeper layers (i.e. several decimetres), such as sedimentation events or bioturbation.

The system [1a] describing the dynamics during daytime emersion periods becomes:

if $\tau > 0$ If $\tau \leq 0$ [2a]

$$\begin{cases} \frac{dS}{dt} = (r_F F = p^b S)(1 - S/S_{max}) - m_S S \\ \frac{dF}{dt} = -r_F F(1 - S/S_{max}) + p^b S(S/S_{max}) - m_F F \\ \frac{d\tau}{dt} = -1 \end{cases} \qquad \begin{cases} \frac{dS}{dt} = -r_S S - m_S S \\ \frac{dF}{dt} = +r_S S - m_F F \\ \frac{d\tau}{dt} = -1 \end{cases}$$

The system [1b], describing the dynamics during night emersion periods, becomes:

$$\begin{cases} \frac{dS}{dt} = -r_S S - \mu_S S \\ \frac{dF}{dt} = +r_S S - \mu_F F \\ \tau = \tau_0 \end{cases} \qquad [2b]$$

And the system [1c], describing the dynamics during submersion periods, becomes:

$$\begin{cases} S = 0 \\ \frac{dF}{dt} = -\nu_F F \\ \tau = \tau_0 \end{cases} \qquad [2c]$$

Where p^b is the production rate (T^{-1}); during daytime emersion periods, the flux of biomass, from S to F, which exists even if the net vertical migration is oriented upward, is represented by the term: $p^b S(S/S_{max})$ and reaches a maximum when $S = S_{max}$. This

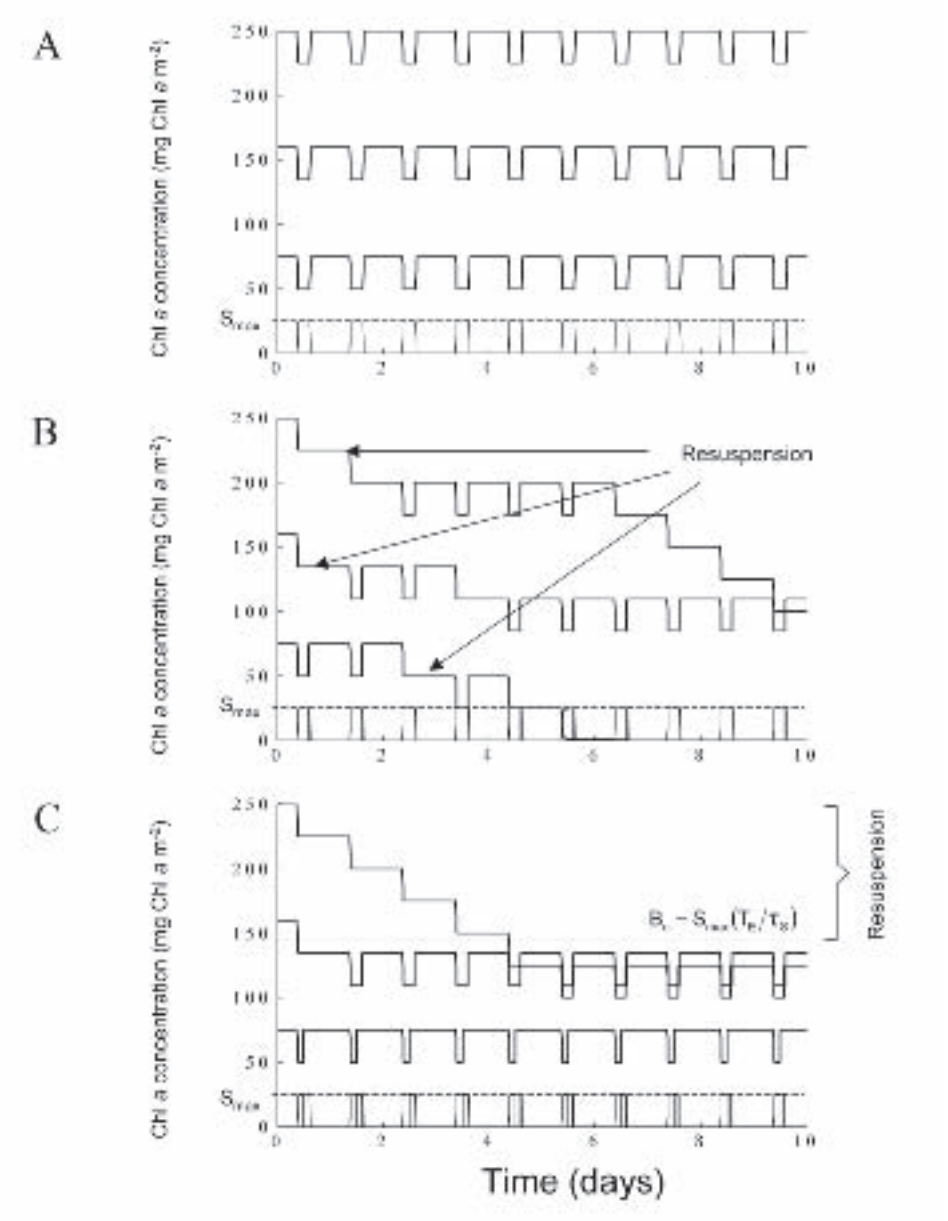

Figure 4. Simulations of vertical migration rhythm and net exchanges between S and F. At the beginning of each daytime emersion period, S (thin line) increased rapidly from 0 to S_{max}, and F (bold line) decreased from F_0 to (F_0-S_{max}). When each daytime emersion ends, S decreased rapidly from S_{max} to 0, when it is transferred into F or was resuspended into the overlying water at the beginning of a submersion. Three hypotheses were tested. A) no resuspension. B) random resuspension C) resuspension above a critical value for the overall biomass B_c. For each case, 3 initial values for F were chosen, 250, 160 and 75 mg Chl a m^{-2}. The 9 simulations were performed independently.

flux term allows production to happen even if the productive layer (S) is saturated, and furthermore, it implies that there is a constant renewal of cells at the mud surface during a daytime emersion period. m_S, μ_S, m_F, μ_F and ν_F are the loss rates (T^{-1}) for S and F and for each of the three different periods.

Modelling the microphytobenthos environment

The main environmental variables that affect the dynamics of the microphytobenthos in the model are hydrodynamic (water height and current velocities). The hydrodynamic variables control the alternating emersion and submersion periods, the light irradiance and the mud temperature, all of which synchronize and control the production in the biofilm at the mud surface during daytime emersion periods. Light irradiance changes the energy balance, and hence the mud surface temperature during daytime emersion periods. All these variables have been linked and represented in one single deterministic model formulation (Figure 5).

Hydrodynamics: The shallow-water hydrodynamic model is based on depth-averaged Navier-Stokes equations with hydrostatic and Boussinesq approximations (*i.e.* the fluid is considered to be incompressible). It simulates horizontal averaged velocities (u,v, in $m.s^{-1}$) and free-surface elevation ζ (m):

$$\begin{cases} \dfrac{\partial u}{\partial t} + u\dfrac{\partial u}{\partial x} + v\dfrac{\partial u}{\partial y} - fv = -g\dfrac{\partial \zeta}{\partial x} + \kappa_h\left(\dfrac{\partial^2 u}{\partial x^2} + \dfrac{\partial^2 u}{\partial y^2}\right) + \dfrac{\omega_x^w - \omega_x^f}{\rho(h+\zeta)} \\ \dfrac{\partial v}{\partial t} + u\dfrac{\partial v}{\partial x} + v\dfrac{\partial v}{\partial y} + fu = -g\dfrac{\partial \zeta}{\partial y} + \kappa_h\left(\dfrac{\partial^2 v}{\partial x^2} + \dfrac{\partial^2 v}{\partial y^2}\right) + \dfrac{\omega_y^w - \omega_y^f}{\rho(h+\zeta)} \\ \dfrac{\partial z}{\partial t} + \dfrac{\partial u(h+\zeta)}{\partial x} + \dfrac{\partial v(h+\zeta)}{\partial y} = 0 \end{cases}$$

where g represents the gravity ($m.s^{-2}$), f, the coriolis factor (s^{-1}), h the water height at the Lower Low Water (LLW water height for a tidal coefficient equal to 20), and ρ, the water density ($kg.m^{-3}$). κ_h is the diffusion coefficient ($m^2.s^{-1}$). ω^W and ω^f are the shear stress ($kg.m^{-1}.s^{-2}$) induced by basin bottom and wind, respectively and they are defined for directions x and y for the calculation of u and v respectively.

This model is minimal (*i.e.* it takes into account only the most essential processes to describe the dynamics) for any shallow water ecosystem where the vertical mixing is strong enough to prevent vertical gradients from developing. The tidal oscillation is induced by the open coastal boundary conditions that are only given in elevation, ζ, (Dirichlet boundary conditions). The two main first harmonic components of the tidal oscillations (M2 and S2) were included to describe the tide in the Marennes-Oléron Bay. They contribute respectively, and on average: 3.2 and 0.4 m to the tidal range, with a periodicity equal to 12H25 and 24H50 and a phase equal to 6.108 and 1.745 radians.

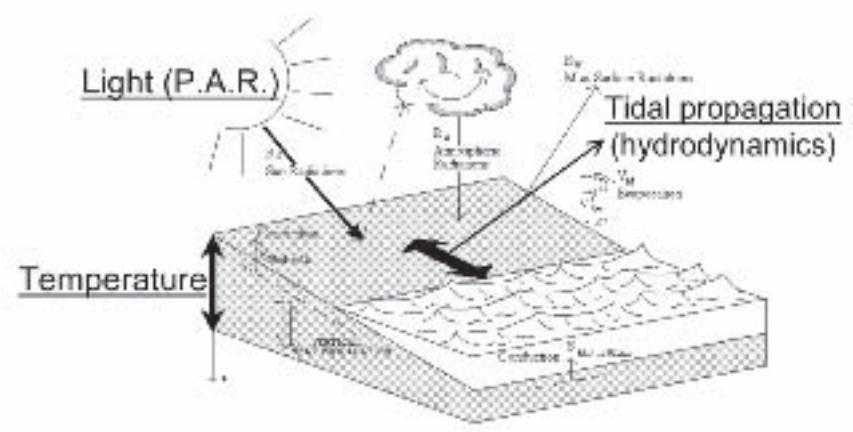

Figure 5. Conceptual scheme for the representation of the forcing synchronizers and factors influencing the production (tidal propagation, incident light irradiance and mud surface temperature). These three components are linked and were represented in the same deterministic model.

An Alternating Direction Implicit numerical method was used to solve the hydrodynamic equations on a staggered grid (ζ was solved at the middle of each mesh and u and v were solved on the right and upper sides, respectively). This modelling structure does not allow emersion to occur since the term $(h+\zeta)$ in the calculation of the stresses induced by the basin bottom and wind cannot be mathematically equal to zero. Therefore, a minimum water height was arbitrarily set to a small positive value ($(h+\zeta)min = 0.1$ m) which defined the layer of water remaining on the intertidal areas during emersion periods. When this minimum water height is reached, horizontal movements of water toward adjacent meshes are stopped, and consolidated mud (on the ridges) is considered as emerged.

The eulerian residual circulation in the Marennes-Oléron Bay, after a spring to neap tide cycle, is oriented from the north to the south of the ecosystem (Figure 6). Hence, as a general rule, when resuspended particles reach the central channel of the bay, they are quickly transported toward the southern end of the bay, and outside of this semi-enclosed ecosystem.

Incident light energy at the mud surface

The sun light intensity, E_S ($W.m^{-2}$) that reaches the mud surface during daytime emersion is described by the following equation:

$$E_S = E_{max} (\sin(d) \sin(\phi) + \cos(d) \cos(\phi) \cos(AH)) (1-A) (1-\zeta)$$

where E_{max} is the maximum irradiance value ($W.m^{-2}$), d is declination, ϕ is the latitude, AH the true hour angle, A the albedo, and ζ (dimensionless) the light attenuation

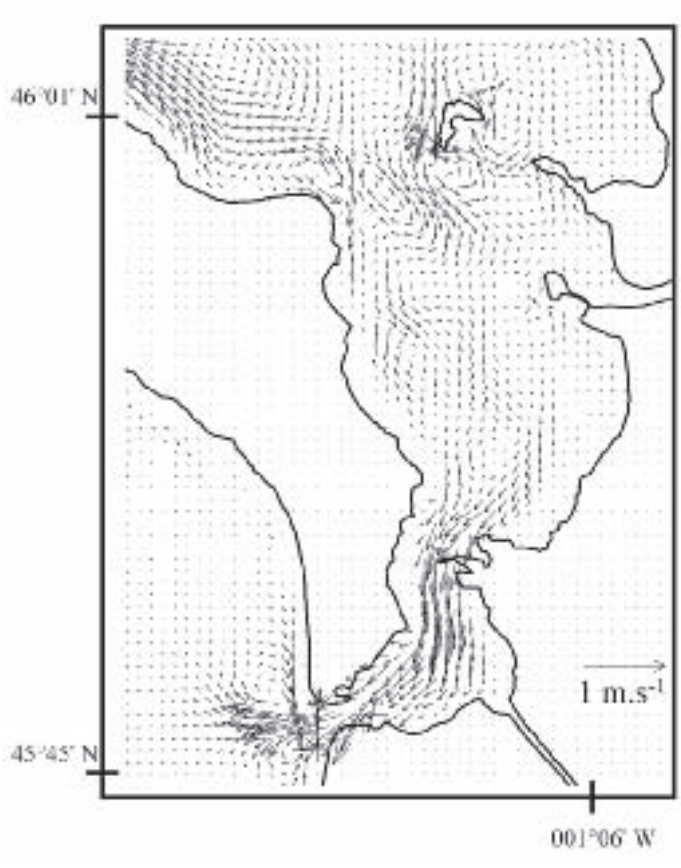

Figure 6. Eulerian Residual circulation in the Marennes-Oléron Bay, calculated from the hydrodynamic model and illustrating the north-south oriented residual flow. The residence time is, on average, 10 days in the bay. However, when particles reach the central channel, they are quickly transported toward the Maumusson Strait, at the southern oceanic boundary of the bay.

due to the cloud cover. According to Frouin (1990), E_{max} is equal to 1358.2 $W.m^{-2}$, between 250 and 4000 nm (total irradiance), and 584.9 $W.m^{-2}$ between 350 and 700 nm (Photosynthethic Active Radiations). E_S is equal to 0 $W.m^{-2}$ during both the night emersion and submersion periods. The light penetration into the mud is so small, that it was neglected in this model.

Temperature of the mud: The mud temperature $T_M(z,t)$ is calculated by the heat vertical propagation equation (Van Boxel 1986):

$$\rho_M C_{P_M} \frac{\partial T_M(z, t)}{\partial t} = \frac{\partial}{\partial z} \eta \frac{\partial T_M(z, t)}{\partial z}$$

where ρ_M is the mud density ($kg.m^{-3}$), C_{P_M}, the mud heat capacity at constant pressure ($J.kg^{-1}.K^{-1}$), η the mud conductivity ($W.m^{-1}.K^{-1}$), t is the time (s) and z the mud depth (m). The boundary conditions at the surface are described by the Heat Energy Balance (HEB, in $W.m^{-2}$) at the mud-air interface during emersion periods (Figure 5):

$$HEB = E_S + R_A - R_M - S_{MA} - V_M$$

Where E_S is the sun light energy flux, R_A the atmospheric radiation energy flux, R_M the mud radiation energy flux, S_{MA} the mud conduction energy flux between mud and air and V_M the evaporation latent energy flux.

During submersion periods, the HEB is described by:

$$HEB = S_{MW} = \frac{\eta}{h_S}(T_M(z_0, t) - T_W(t))$$

where S_{MW} is the mud conduction energy flux between mud and water, η the mud conductivity ($W.m^{-1}.K^{-1}$), h_S the height of the overlying water mixing layer (m) $T_M(z_0, t)$ the mud surface temperature (K) and $T_W(t)$ the water temperature (K). A complete description of the process formulations are available in Guarini *et al*. (1997).

The dynamics of the mud surface temperature (the uppermost centimetre of the mud) is characterized by 3 temporal scales of variations: long term seasonal scale, medium-term scale due to the neap to spring tide cycle (14.6 days) and short-term scale (due to the succession of submersion-emersion periods). Figure 7 represents only the medium-term and short-term variations in summer, when the MST variations are at a maximum. The highest MST (around 40 °C) are reached in Summer during spring tide – when low tide corresponds to midday – in the highest part of the mudflat. However, meteorological variability can hide neap to spring tide medium-term variations (Guarini *et al*. 1997).

Primary production processes

Production vs. Photosynthetic Active Radiations

The production rate is estimated by the photosynthetic activity, which was studied experimentally as a function of the photosynthetic active radiations, PAR, (Blanchard and Cariou-Le Gall 1994) and temperature (Blanchard *et al*. 1997). Experiments realized under controlled conditions, reflect the potential photosynthetic activity of the microphytobenthos. Microphytobenthos were separated from sediment exploiting their active vertical migration, according to the method developed by Couch (1989), and were then studied as a suspension of phytoplankton cells, in seawater. Primary production was estimated in terms of carbon assimilation, using ^{14}C labelling techniques

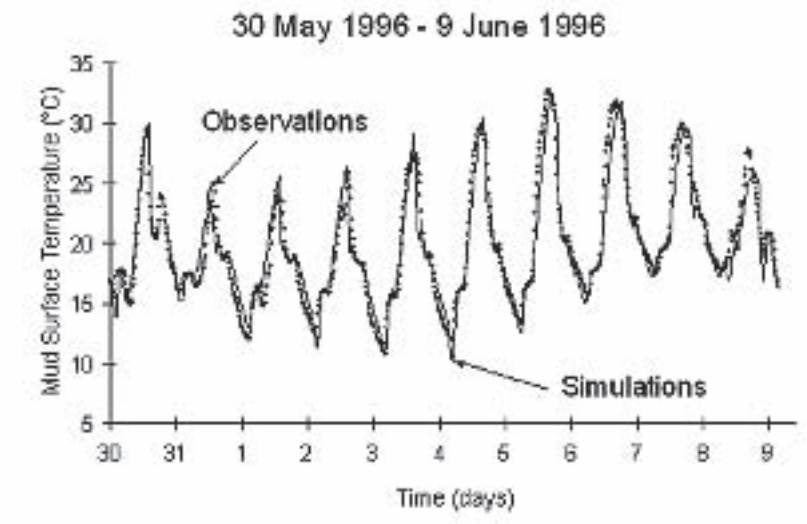

Figure 7. Mud surface Temperature (MST) variations during a neap-to-spring tide cycle. The MST was recorded during 11 days in early June 1996 and observations (dots) were compared to the simulations (line). The model predicts the MST with a precision of ca. 1 °C. During a tidal cycle, the MST dynamics is characterized by a sharp increase during daytime emersion, and a slower decrease during night emersion. During the submersion period, the MST reaches quickly an equilibrium with the water temperature.

(Blanchard *et al*. 1997). Since the incubation time used in the experiments was on the order of hours, any short-term changes that occur on the timescale of minutes were not taken into account. The experimental results showed an initial increase in the photosynthetic activity from 0 h^{-1} at 0 $W.m^{-2}$, with a slope α^b, which represents the photosynthetic efficiency. When the PAR increased, the curve converged to an asymptotic value, p^b_{max}, which represents the photosynthetic capacity of the microalgal community. Based on these results, the chl*a* normalized photosynthetic activity (h^{-1}) was described as a function of light energy by the following formulation:

$$p^b = p^b_{max} \tanh\left(\frac{E}{E_k}\right) = p^b_{max} \tanh\left(\frac{\alpha b E}{p^b_{max}}\right)$$

where p^b_{max} is the photosynthetic capacity (h^{-1}) and corresponds to the maximum asymptotic value of the P-E curve. E_k is the intersection between the slope at the origin (α^b, in J m^{-2} also called the photosynthetic efficiency) and the asymptotic value $p^b = p^b_{max}$ (h^{-1}). The seasonal evolution was characterized by a constant estimated value for E_k, which remained close to 100 $W.m^{-2}$ (Figure 8).

Maximum production vs. Photosynthetic Active Radiations

The asymptotic value, p^b_{max} or the photosynthetic capacity (h^{-1}), estimates the maximum production for a given environmental condition that varies with temperature.

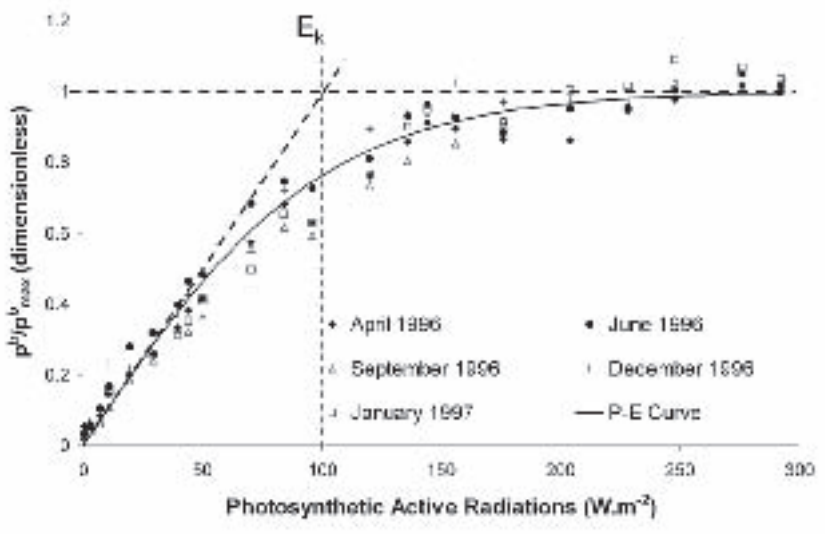

Figure 8. Standardized P-E curves. Photosynthetic activities were measured experimentally as a function of the Photosynthetic Active Radiations (PAR) using a ^{14}C assimilation method. The seasonal pattern is characterized by a constant value for E_k suggesting that the microphytobenthos did not acclimate to its light environment. E_k is estimated at around 100 $W.m^{-2}$, and most of the time, during daytime emersion periods, the microphytobenthos receives a saturating light for photosynthesis.

p^b_{max} increases when temperature increases up a maximum value which is the optimal value for photosynthesis, and then decreases down to zero until the maximum (or lethal) temperature for the photosynthesis is reached. The relationship between the photosynthetic capacity, p^b_{max} (h^{-1}), and the temperature T (°C) is described by the following formulation:

$$p^b_{max} = p^b_{max}(\varepsilon_T)^{\beta}\exp\{\beta(1-\varepsilon_T)\}$$

where β is the curvature coefficient of the curve, and ε_T is the relative deviation of the temperature T (°C) from the maximum value T_{max} (°C):

$$\varepsilon_T = \left(\frac{T_{max} - T}{T_{max} - T_{opt}}\right)$$

where, T_{opt} (°K) is the optimal temperature for the photosynthesis. The relationship between p^b_{max} and temperature was studied seasonally (Blanchard *et al*. 1997). The relationship was characterised by stable optimal and maximum temperatures for photosynthesis (Figure 9); only the maximum photosynthetic capacity varied showing a maximum in spring (of about 0.3 h^{-1}) and a minimum in winter (of about 0.1 h^{-1}).

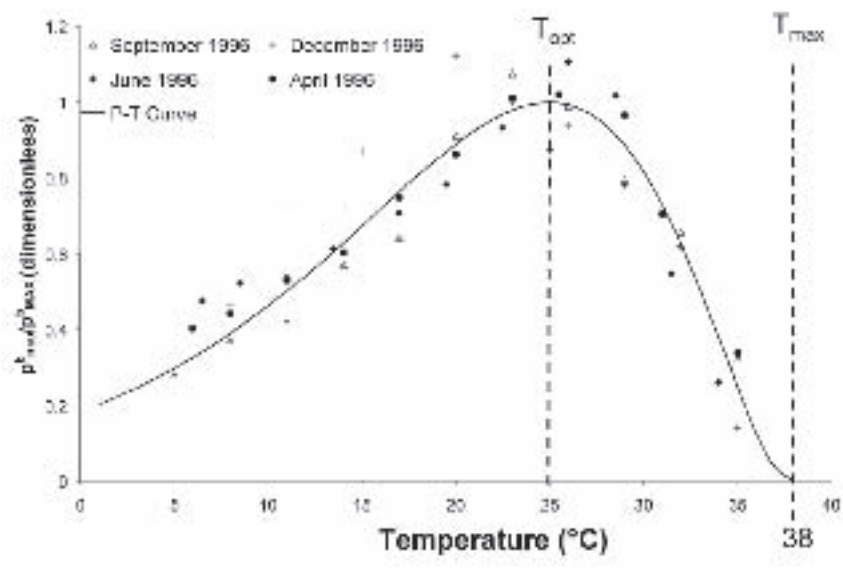

Figure 9. Standardized P-T curves. Photosynthetic capacity was measured experimentally as a function of the temperature (in the range of the field mud surface temperature variability) using a ^{14}C assimilation method. The seasonal pattern is characterized by a constant value for the optimal (T_{opt}=25 °C) and maximum (T_{max}=38 °C) temperature for the photosynthesis. The curvature coefficient did not differ significantly either. This suggested that the microphytobenthos did not present any acclimation to its thermal environment.

In order to quantify the influence of the mud surface temperature on the productivity of the microphytobenthos, the photosynthetic capacity was calculated as a function of the mud surface temperature, using the model that represents the photic, thermal, and hydrodynamic environment in the Marennes-Oléron Bay. Interestingly, during summer, the mud surface temperature reached a maximum of ca. 38 °C and is frequently above the optimal temperature for photosynthesis of 25 °C. Figure 10 shows that at the low tide of a spring tide in summer, the microphytobenthos is thermo-inhibited over most intertidal areas in Marennes-Oléron Bay: 75 % of the total intertidal area is affected by the phenomenon of thermo-inhibition at spring tide and 20 % at neap tide. In summer, microalgae undergo fast and large variations of temperature (from 18 °C at the beginning of the daytime emersion period, to 36 °C after 6 hours of emersion), which are unavoidable even by downward migration into the sediment, since the temperature increase propagates more than one centimetre deep into the mud during an emersion period (Harrison and Phizacklea 1987, Guarini *et al*. 1997). The microphytobenthos does not adjust its optimal photosynthetic capacity (p^b_{max}) to the seasonal changes in the maximum temperature reached at the surface of the intertidal mudflat. This lack of temperature acclimation may be due to the rapidity of the temperature increase during daytime emersion periods.

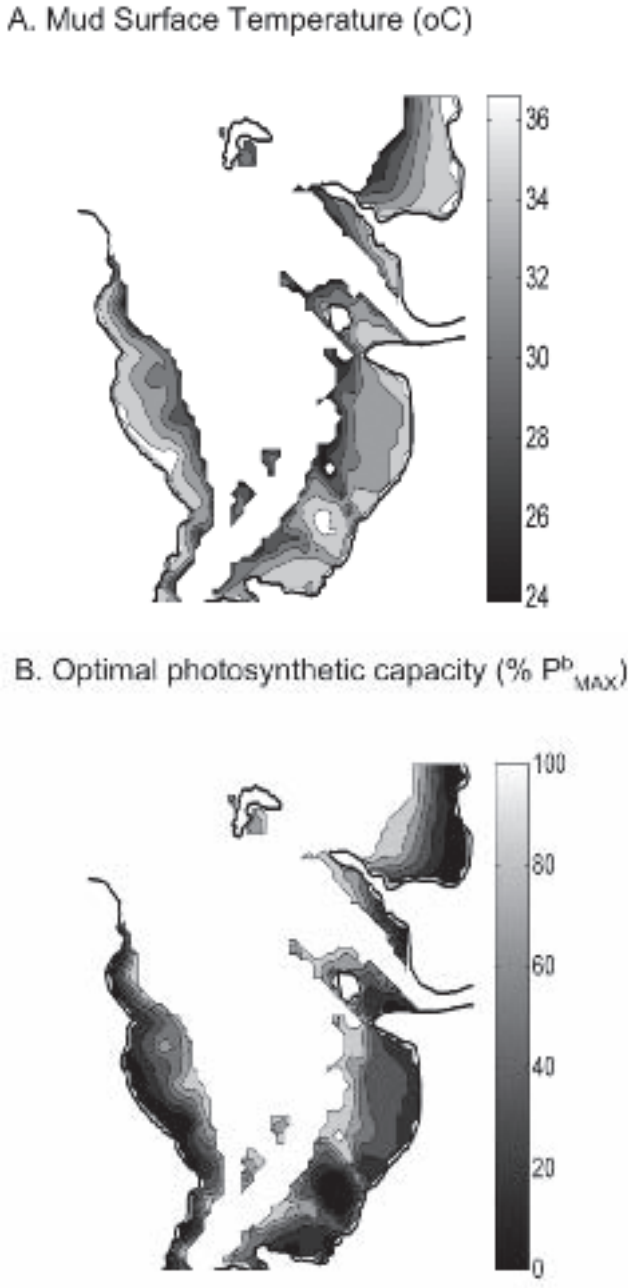

Figure 10. Simulation of the Mud Surface Temperature (MST °C) and the photosynthetic capacity (as a percentage of the maximum value) in the Marennes-Oléron Bay in summer (June, day 182). Results are for a low tide at spring tide. The MST temperature increased up to 36 °C and was above the optimal temperature for the photosynthesis (Topt = 25 °C) over 80 % of the total area. The result is a general thermo-inhibition of the microphytobenthic productivity in the intertidal mudflats of the Marennes-Oléron Bay

Dynamic changes of the photosynthetic activity – photo-inhibition vs. photo-acclimatation

The photosynthetic activity varies not only as a function of light and temperature but also as a function of the ecophysiological state of the microalgal community. Two opposite reactions, photo-acclimation and photo-inhibition, occur when a long exposure to saturating light radiation affects the photo-systems of the microalgae. Photo-acclimation is a process that requires a physiological adjustment of the cells, which is difficult to achieve in a rapidly fluctuating environment. Photo-inhibition is a reaction to strong light irradiance, which provokes a decrease of photosynthesis, without changes in pigment concentration. Cells switch instantaneously from dark to saturating light for photosynthesis during daytime emersion and photo-inhibition is more likely to happen at the mud surface when microalgae are exposed to a saturating PAR, suddenly and for several hours.

The photo-inhibition process was studied experimentally (Blanchard *et al*. submitted) by exposing suspensions of benthic microalgae to a saturating light for the photosynthesis and at constant temperature; P-E curves were measured at regular time intervals (every 30 min). The Jassby and Platt (1976) equation was used to estimate the parameters: α^b (photosynthetic efficiency), E_k (light irradiance at saturation), and p^b_{max} (the photosynthetic activity).

The photo-inhibition process (Figure 11) was described by the following dynamic system:

$$\begin{cases} \dfrac{dp^b_{max}}{dt} = \gamma\left(p^b_{opt} - p^b_{max}\right) \\ \dfrac{dp^b_{opt}}{dt} = -p^b_{opt}\,\dfrac{(\delta + 1)}{t_{ph}}\left(\dfrac{t}{t_{ph}}\right)^d \\ \dfrac{dE_k}{dt} = \kappa(E_{max} - E_k) \end{cases}$$

which also determines the temporal evolution of $\alpha^b = \dfrac{p^b_{max}}{E_k}$

where p^b_{opt} (h^{-1}) is the optimal value of p^b_{max}, τ_{ph} (h) is the time threshold from which p^b_{opt} begins to decrease, γ (h^{-1}) the rate for p^b_{max} to converge towards its maximum value p^b_{opt}, δ is a dimensionless parameter representing the intensity of photo-inhibition, κ (h^{-1}) is the fitting rate to new saturating light conditions that leads to the maximum light irradiance at saturation, E_{max} ($W.m^{-2}$).

It has been suggested that photo-inhibition does not occur in intertidal mudflats, not only because the pattern which was characterised experimentally was not observed in the field, but also because the microalgae can migrate quickly down to aphotic conditions (in few hundred micrometers). This constant renewal of the biofilm, already suggested by Blanchard and Cariou-Le Gall (1994), is consistent with an increase of the overall biomass in the first centimetre of the mud during daytime emersion periods, even if the biofilm reaches its maximum cell density at the mud

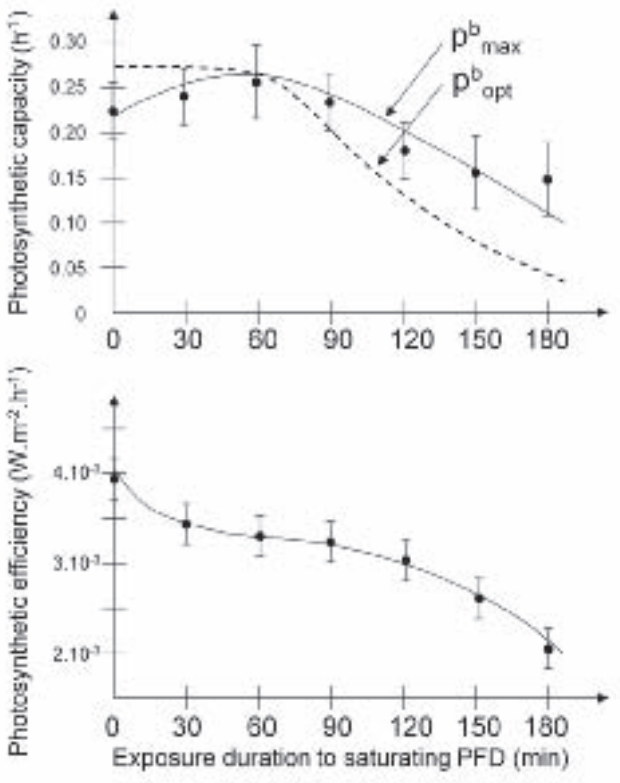

Figure 11. Measured and simulated photo-inhibition. The photo-inhibition of the microphytobenthic productivity was induced experimentally by maintaining a suspension of extracted cells in saturating light for the photosynthesis. The photosynthetic capacity and the photosynthetic efficiency were estimated every 30 min. during 180 min. The optimal value for the photosynthetic capacity is estimated from a dynamic model. Photo-inhibition (a decrease of the optimal photosynthetic capacity) started after ca. 1 hour of saturating light exposure.

surface. Thus, in the dynamic model, which describes the dynamic of the microphytobenthos biomass, the time spent by a group of cells (or by a unit of biomass) at the mud surface is considered as less than the time that is necessary to induce photo-inhibition when cells are exposed to saturating PAR The order of magnitude of this time, τ_s, is about 1 hour (Figure 11).

Mathematical properties of the dynamical model

Slow-Fast formulation

The first step in studying the mathematical properties of the system is to differentiate the dynamics into two temporal scales, qualified as ‘slow’ and ‘fast’. The model parameters

are S_{max}, r_F, r_S, p^b, m_S, m_F, μ_S and μ_F. S_{max} has the same unit as the state variables S and F (mg Chl *a* m^{-2}) and its estimated value is 25 (mg Chl *a*) m^{-2}. The other parameters are standardized rates (1/time unit) and can be ranked, according to their typical order of magnitude, from the highest value to the lowest:

$$r_S\,(100) \gg r_F\,(10) \gg p\,(1) \gg (m_S \approx m_F \approx \mu_S \approx \mu_F \approx \nu_F)\,(0.1)$$

In addition, a transformation can be applied to the model: B = S+F. This transformation is particularly valuable since B can be sampled easily on a mudflat, even while it remains difficult to observe the biomasses S and F separately. The model then becomes:

During daytime emersion periods:

if $\tau > 0$ If $\tau \leq 0$ [3a]

$$\begin{cases} \dfrac{dS}{dt} = \left(r_F(B - S) + p^b S\right)\left(1 - S/S_{max}\right) - m_S S \\ \dfrac{dB}{dt} = \left(p^b - m_S + m_F\right)S - m_F B \\ \dfrac{d\tau}{dt} = -1 \end{cases} \qquad \begin{cases} \dfrac{dS}{dt} = -r_S S - m_S S \\ \dfrac{dB}{dt} = (m_F - m_S)\,S - m_F B \\ \dfrac{d\tau}{dt} = -1 \end{cases}$$

During night emersion periods:

$$\begin{cases} \dfrac{dS}{dt} = -r_S S - \mu_S S \\ \dfrac{dB}{dt} = (\mu_F - \mu_S)S - \mu_F B \\ \tau = \tau_0 \end{cases} \qquad [3b]$$

During submersion periods:

$$\begin{cases} S = 0 \\ \dfrac{dB}{dt} = -\nu_F B \\ \tau = \tau_0 \end{cases} \qquad [3c]$$

These systems of equations describe slow-fast systems where S is the fast variable and B the slow one. Variations of S depend on fast processes (upward and downward migration) whereas variations of B only depend on slow processes (production and loss terms). The system can now be studied at these two scales of variation.

First, to examine variations at the fast-time scale the slow motions are "frozen" and the processes of production and loss terms become negligible relative to the vertical migrations. The model is then simplified by:

During daytime emersion periods:

if $\tau > 0$ If $\tau \leq 0$ [4a]

$$\begin{cases} \frac{dS}{dt} \approx r_F(B - S)(1 - S/S_{max}) \\ \frac{dB}{dt} \approx 0 \\ \frac{d\tau}{dt} = -1 \end{cases} \qquad \begin{cases} \frac{dS}{dt} \approx -r_S S \\ \frac{dB}{dt} \approx 0 \\ \frac{d\tau}{dt} = -1 \end{cases}$$

During night emersion periods:

$$\begin{cases} \frac{dS}{dt} \approx -r_S S \\ \frac{dB}{dt} \approx 0 \\ \tau = \tau_0 \end{cases} \quad [4b]$$

During submersion periods:

$$\begin{cases} S = 0 \\ \frac{dB}{dt} \approx 0 \\ \tau = \tau_0 \end{cases} \quad [4c]$$

For a short time, t, it is only possible to observe a variation in S; this happens during the daytime emersion periods (according to the condition that was set for τ) and at the beginning of the night emersion periods only. No variation in S is observed during the immersion periods. The sets of stationary points (L) of the fast equations are defined when dS/dt = 0, providing the "slow curves" of the systems. During the daytime emersion period, when $\tau > 0$, the slow curve is:

$$L_1 = \{(S,B) \in \mathbb{R}^+ \times [S_{max}, +\infty] / S = S_{max}\}$$

The condition $B \geq S_{max}$ ensures that the biomass content of the F-compartment is sufficient to fill up the biofilm at the mud surface. The domain of the definition is restricted to $[S_{max}, +\infty]$.

During the daytime emersion period, when $\tau \leq 0$, and during night emersion and submersion periods, the slow curve is described by:

$$L_2 = \{(S,B) \in \mathbb{R}^+ \times \mathbb{R}^+ / S = 0\}$$

Secondly, at the slow-time scale, fast motions appear instantaneous and at the beginning of each daytime emersion period, S 'jumps' from 0 to S_{max}, into the slow curves L_1. During daytime emersion period (when $\tau \leq 0$), night emersion or submersion period, S jumps from S_{max} to 0, if it is not already equal to 0, corresponding to the slow curve L_2. At this slow-time scale, and for limited period of time (*e.g.* a few neap-to-spring tide cycles), it can be assumed that the loss rates affecting S at the mud surface are not different locally from the loss rates affecting F at the sub-surface, and hence, $m_F \approx m_S \approx m$ during the daytime emersion period and $\mu_F \approx \mu_S \approx \mu$ during night emersion periods (m and μ affect B). The loss rates, ν_F, affecting F during submersion periods were also renamed ν, and represent the loss rates which affect B, consistent with the two previous simplifications. The simplified systems at a slow-time scale are:

During daytime emersion periods:

if $\tau > 0$, $S=S_{max}$ If $\tau \leq 0$, $S=0$ [5a]

$$\begin{cases} \frac{dS}{dt} \approx 0 \\ \frac{dB}{dt} \approx p^b S_{max} - mB \\ \frac{d\tau}{dt} = -1 \end{cases} \qquad \begin{cases} \frac{dS}{dt} \approx 0 \\ \frac{dB}{dt} \approx -mB \\ \frac{d\tau}{dt} = -1 \end{cases}$$

During night emersion periods:

$$\begin{cases} \frac{dS}{dt} \approx 0 \\ \frac{dB}{dt} \approx -\mu B \\ \tau = \tau_0 \end{cases} \quad [5b]$$

During submersion periods:

$$\begin{cases} S = 0 \\ \frac{dB}{dt} \approx -\nu B \\ \tau = \tau_0 \end{cases} \quad [5c]$$

During the daytime emersion periods, as long as $\tau > 0$, the production is described as a proportion of the constant biomass S_{max}. Then, the biomass B increases along the slow curve L_1 and converges asymptotically toward the equilibrium value $B^* \approx p^b S_{max} / m$ where m is the mortality rate during daytime emersion (h^{-1}); the smaller m becomes, the higher B* is. For $\tau \leq 0$ or during the night emersion and submersion periods, B decreases along the slow curve L_2 and converges asymptotically down to

the equilibrium value B*≈0, which represents the extinction of the microphytobenthos. The dynamics of the variable B are governed by the periodic succession of the four sub-systems of ordinary differential equations.

Mathematical behaviour of the system

Each sub-system (Equations 5a, 5b, 5c) was integrated analytically. The number of parameters is reduced by assessing that, locally, the loss rates are not significantly different where m = (m ≈ μ ≈ ν). In addition, the two sub-systems that described the dynamics of the microphytobenthos during a daytime emersion period were combined in one integrated equation. Therefore, three integrated equations described the evolution of the system at the slow time-scale:

During daytime emersion periods:

$$B_E = B_{E_0} e^{-mT_E} + \frac{p^b S_{max}}{m} e^{-m(1-\alpha)(T_E-T_P)} - \frac{p^b S_{max}}{m} e^{-mT_E}$$

During night emersion periods:

$$B_N = B_{N_0} e^{-mT_N}$$

During submersion periods:

$$B_I = \left(B_{I_0} - \alpha S_{max}\right) e^{-mT_I}$$

where T_E, T_P, T_N and T_I are the durations of the daytime emersion period, the production period (corresponding to the presence of the biofilm at the mud surface), the night emersion period and the submersion period respectively, and with $\alpha=0$ if $T_P<T_E$ and $\alpha=1$ if $T_P \geq T_E$. If $\alpha=0$, no resuspension occurs, if $\alpha=1$ and the submersion period follows a daytime emersion period, S_{max} is resuspended in the water column.

The first and second hypotheses (Figure 12A,B) assume that the duration of the biofilm is synchronized with the duration of the daytime emersion period. In the first case, the synchronization is exact and the migration phases correspond to the beginning and the end of each daytime emersion period. In the second case, some fluctuations in the duration may induce resuspension randomly when the reflood occurs before the expected (deterministic) moment. In both cases $T_E \approx T_P$, and without any random fluctuations on the duration of the period T_E, $\alpha=0$. The solution for a typical succession (1-periodic case) of the following periods (Daytime E.+Submersion+Night E.+Submersion) is then:

$$B_I^{n+1} = (e^{-mT}) B_I^n + \frac{p^b S_{max}}{m}\left(1 - e^{-mT_E}\right) e^{-m(T-T_E)} - \alpha S_{max} e^{-m(T-T_E)}$$

$$B_E^{n+1} = (e^{-mt}) B_E^n + \frac{p^b S_{max}}{m}\left(1 - e^{-mT_E}\right) - \alpha S_{max} e^{-mT}$$

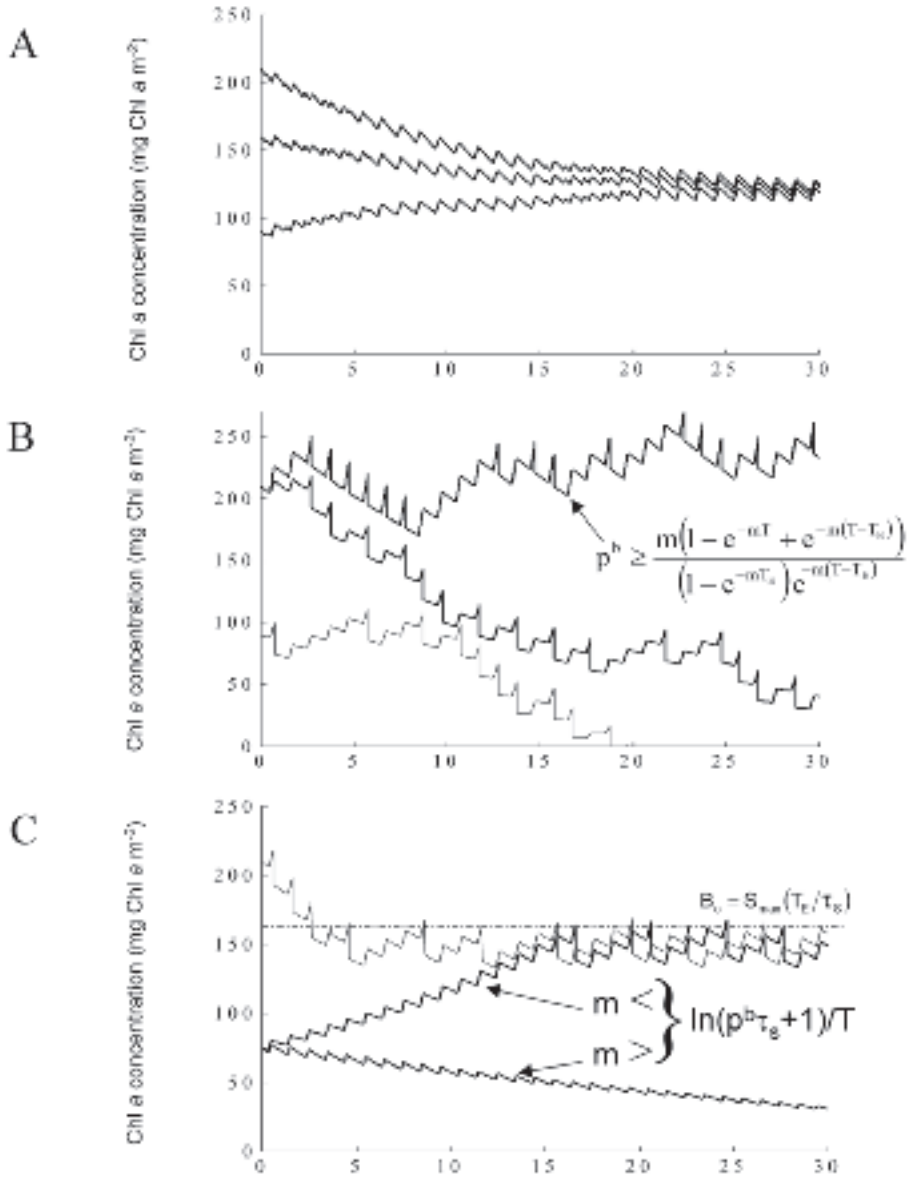

Figure 12. Simulations of the dynamics of the microphytobenthic biomass. The overall biomass (B=S+F) is represented in term of chlorophyll *a* concentration. The three figures A, B and C correspond to the three hypotheses that were tested for the vertical migration (see Figure 4). A) The chlorophyll *a* concentration converges to a unique positive, stable steady state condition. B) The chlorophyll *a* concentration converges to a positive, stable steady state according to the balance between the productivity and the global losses (grazing, natural mortality). C) The chlorophyll a concentration converges to the critical concentration $B_c=S_{max}(T_E/\tau_S)$, if the loss rates are lower than $(1/T)\ln(p^b\tau_s+1)$. Otherwise, it decreases down to zero. The steady state cycle is sensitive to the value of the initial condition.

with $T = T_I+T_N+T_I+T_E = 24h$. The discrete time series $B^{n+1} = aB^n + b$, where $a < 1$, converges to stable steady states ($B^* = b/(1-a)$), which are respectively:

$$B^*_I = \frac{\left((p^b/m)(1 - e^{-mT_E}) - \alpha\right) S_{max} e^{-m(T-T_E)}}{(1 - e^{-mT})}$$

and,

$$B^*_E = \frac{\left((p^b/m)(1 - e^{-mT_E}) - \alpha e^{-mT}\right) S_{max}}{(1 - e^{-mT})}$$

The steady state of the biomass dynamics is thus characterized by a series of oscillations, and the amplitude of these oscillations at steady state is equal to:

$$\Delta B^* = B^*_E - B^*_N = \frac{S_{max}}{(1 - e^{-mT})} \left(\frac{p^b}{m} (1 - e^{-mT_E})(1 - e^{-m(T-T_E)}) + \alpha e^{-mT} (e^{mT_E} - 1) \right)$$

The amplitude is always positive and is defined as long as m is greater than zero. The period T is always greater than T_E. If $\alpha=0$, no resuspension of the microalgal biomass occurs and the biomass converges to a series of positive steady state values. On the contrary, if α alternates randomly between 0 and 1, there is an episodic resuspension of the biofilm and the biomass deviates from the series of steady state values. If α is always equal to 1, there is a constant resuspension of the biofilm, and p must respect the following inequality to ensure that the biomass will maintain a minimum steady state value greater than S_{max}:

$$pb \geq \frac{m\left(1 - e^{-mT} + e^{-m(T-T_E)}\right)}{(1 - e^{-mT_E}) e^{-m(T-T_E)}}$$

Similar calculations can be performed using a more realistic case with a changing phase difference between the tidal and light-dark cycles over a 15 day period (15-periodic case). The conclusions remain the same (Guarini *et al*. 2000b) since the dynamics of the biomass can by described by a similar series $B_{n+1} = aB_n + b$ where $a = \exp(-mT) < 1$. The biomass again converges to a series of steady state values $B^* = b/(1-a)$, where b can be calculated at the beginning of each daytime emersion, night emersion and submersion period. Finally, the model accounts for variations in p^b as a function of both incident light irradiance and mud surface temperature. In this case, p^b is replaced by $p^b(t) = p^b_{MAX}.f(t)$ with f(t), a periodic function of the time t, which limits the maximum production rate p^b_{MAX}. During daytime emersion period, the total biomass increases, from an initial value B_0, to reach the value, B_E:

$$B_E = e^{-mT_E} B_0 - e^{-mT_E} p^b_{MAX} S_{max} \int_{T_E} f(t) e^{mt} dt$$

For any sequence or combination of daytime emersion, night emersion and submersion periods, the dynamics can be described by a numerical series $B_{n+1} = aB_n + b$.

b includes the integral of the function of production (f(t)exp{mt}), which can be integrated numerically. a = exp(-mT) < 1, ensures that the numerical series converge to steady state series of values B* = b/(1-a). For any set of positive parameters, and according to the assumptions that we made, the model converges toward a series of steady state values whatever the frequency of the environmental synchronizers is.

The third hypothesis (Figure 12C) assumes that the duration of the biofilm at the mud surface during daytime emersion period is determined by the initial amount of biomass able to migrate. In the model, this initial biomass is B_0, which is also equal to F_0 since there is no biofilm at the mud surface, at the beginning of the daytime emersion. The potential duration of the biofilm is given by τ_0. It is calculated by dividing the initial biomass by S_{max}, and by multiplying this value by the average time spent by a unit of biomass (equal to S_{max}) at the surface of the mud: $\tau_0 = \tau_s \times (B_0/S_{max}) = \tau_s \times (F_0/S_{max})$. From these estimates, and using T_E, the duration of the daytime emersion period, the critical biomass for resuspension was calculated, $B_c = S_{max} \times (T_E/\tau_s)$. In the theoretical 1-day periodicity, for the case of the succession of the sequence (Daytime E.+Submersion+Night E.+Submersion) with a period T = 1 day, the discrete model is equal to:

$$B_{n+1} = B_n e^{-mT_E} + \frac{S_{max}p^b}{m} e^{-m(1-\alpha)(T_E-T_P)} e^{-m(T-T_E)} - \frac{S_{max}p^b}{m} e^{-mT} - \alpha S_{max} e^{-m(T-T_E)}$$

Two cases were investigated: when $\alpha = 1$, B is greater than B_c and the biofilm is resuspended in the water column each time the submersion period follows the daytime emersion period. When $\alpha = 0$, B is lower than B_c and there is no resuspension at all.

When $\alpha = 1$, $B_0 \geq B_c$, the series can be summarized by $B_{n+1} = aB_n + b$ where $a = \exp(-mT_E) < 1$. Therefore, the biomass converges to a series of steady state values B* = b/(1-a), which are given by:

$$B^* = S_{max} e^{mT_E} \left(\frac{p^b}{m} - \frac{p^b}{m} e^{-mT_E} - 1 \right) \Big/ (e^{mT} - 1)$$

which decreases lower than B_c if :

$$p^b < \frac{m\left(T_E e^{mT} - T_E + \tau_S e^{mT_E}\right)}{\tau_S (e^{mT_E} - 1)}$$

When $\alpha = 0$, $B_0 < B_c$, the model has a more complex behaviour. The numerical series:

$$B_{n+1} = B_n e^{-mT_E} + \frac{S_{max}p^b}{m} e^{-mT} (e^{m\tau_S B_n} - 1)$$

increases if,

$$p^b > \frac{(e^{mT} - 1)}{\tau_S} \text{ or, } m < \frac{1}{T} \ln(p^b \tau_S + 1)$$

and otherwise decreases to zero. According to these different conditions B_c will converge to a unique steady state value (greater than B_c), or to a steady state value that will depend on the initial condition (around B_c), or down to zero, if the grazing is too high to be compensated by the daytime production. As for the previous case, similar calculations can be made in more complicated cases for the 15-periodic case and with a fluctuating production. The complexity becomes higher and the series of coefficients α_j (j= 1, …, 15) are difficult to calculate, because they depends on an increasing number of conditions. Nevertheless, the numerical simulations have shown that the three types of behaviour exist in the model (convergence to a unique cyclic steady state greater than B_c, an initial condition dependant stead-state around B_c, or a local extinction of the microphytobenthos if the grazing is not compensated by the production).

Discussion and perspectives

Definition of the restrictions on the microphytobenthic model. Several conditions must be respected when studying this system. The first condition, $B_c > S_{max}$, ensures that the biomass (F) does not become negative. Two comprehensive surveys (Guarini *et al*. 1998) of the microphytobenthic biomass in the Marennes-Oléron Bay (France) in June 1995 and the other in January 1996 (Figure 13), have shown that the biomass per unit of area and in the first centimetre of the mud (in terms of the chlorophyll a concentration) did not decrease below S_{max}, which was estimated at 25 mg Chl a m^{-2} (Guarini 1998).

The second condition is that the duration of the daytime emersion period does not decrease below $1/r_F$ (where r_F is the biomass transfer rate from F to S) which corresponds to ca. 30 min. In addition, for a numerical purpose, this condition was combined with another condition that assumes that T_E (the duration of the daytime emersion period) has to be greater than τ_S. When this was the case, no vertical migration, no production and mostly no resuspension could occur in the model system. The third condition is that the duration of the daytime emersion period is not greater than the period of the semi-diurnal tidal cycle (12H25). This means that the mud surface is submerged at each tidal cycle. Numerically, the suppression of the submersion period is not problematic (the submersion period and the 'resuspension' coefficient, α, are set to zero), but it induces other problems linked to changes in sediment properties (drying and consolidation) and hence in vertical migration and production of the diatoms. The upper part of the mudflat, which is submerged only during spring tides, was not considered in these simulations.

Sensitivity of the simulations to parameter variability

Sensitivity analyses were performed at steady state, using the typical order of magnitude value of each of the parameters to calculate the nominal solution. The deviation ∂D from the nominal solution, D_0, was calculated at the beginning and at the end of each daytime emersion period, for any variations ∂P_i in each of the initial parameters,

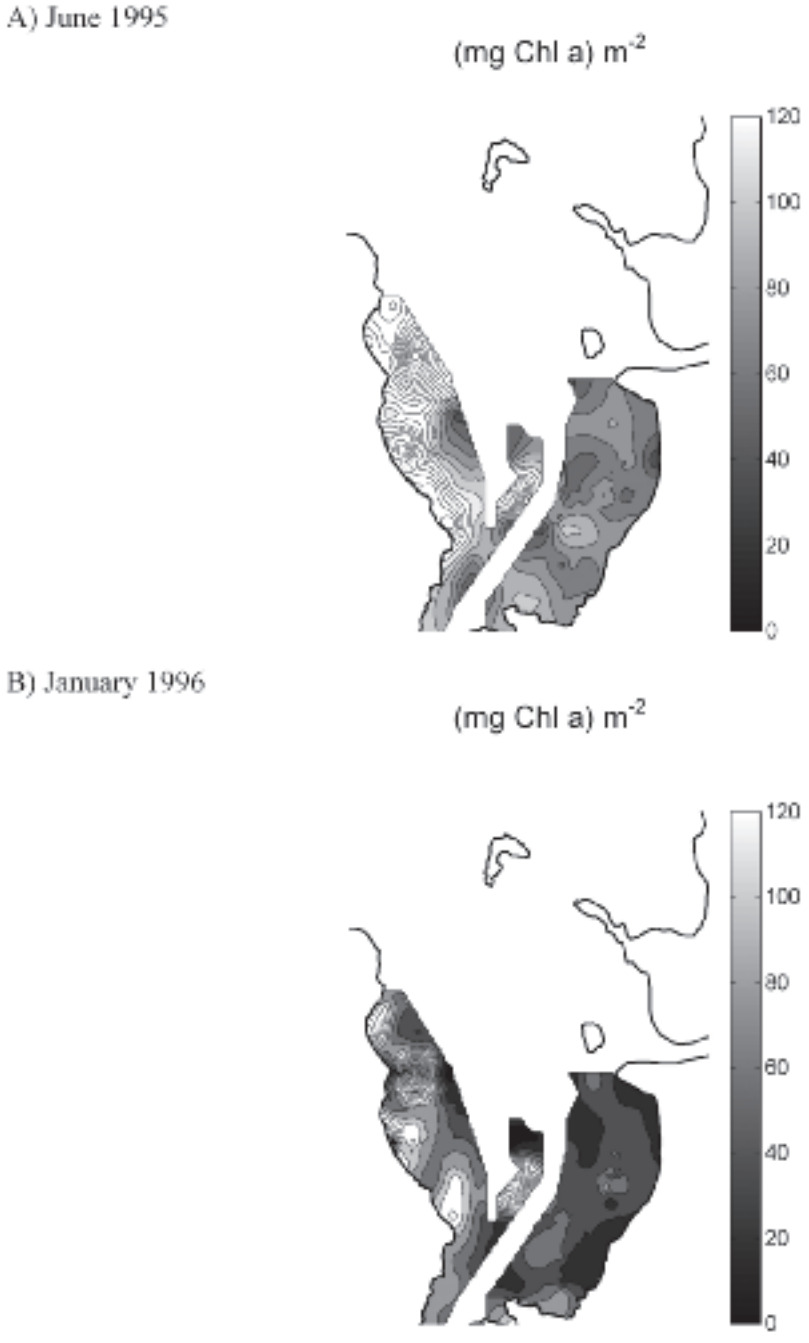

Figure 13. Spatial distribution of the microphytobenthic biomass in term of chlorophyll a concentration in the intertidal mudflats of the Marennes-Oléron Bay. A) Spatial distribution in June 1995, and B) spatial distribution in January 1996.

P_{i0} (Miller, 1974). The first order sensitivity coefficient, S_i, was calculated as a linear deviation from the nominal value: $S_i = \partial D/\partial P_i$. The relative sensitivity coefficients, R_i, were then calculated: $R_i = S_i P_{i0}/D_0$. The simulations were highly sensitive to the parameters p^b, S_{max}, and T_E. The average relative sensitivity coefficients for these parameters were equal to 1.0, meaning that any variations of these parameters have a proportional effect on the steady state estimate (a percentage of variation of these parameters induces the same percentage of variation in the steady state estimate). This justified the efforts made to estimate p^b and S_{max} as a function of the forcing variables and species composition (Guarini 1998); the average relative sensitivity coefficient for τ_s (in the third modelling hypothesis only) was equal to –1.0; T_E and τ_s have an antagonistic effect on the simulations and τ_s has to be estimated accurately.

On the contrary, the sensitivity of the mortality rate is not as high. The average relative sensitivity coefficient for this parameter is equal to -0.5. The main problem with this parameter is not with the sensitivity of the simulations with respect to its variability, but rather with the difficulty in estimating it spatially. Indeed, it depends on a variable, but high number of grazers (from the meio- and macrofauna), as well as on the physiological condition of the microphytobenthic community. It is then necessary to estimate the mortality rate by fitting simulations to observations and in this case, local estimates included a large part of the effect of the variability of the other parameters on the simulated biomass.

Properties of the system

The dynamics of the microphytobenthic biomass in the first centimetre of the mud (B), as it is described in the model, is characterized by a series of strong oscillations which can be observed at the beginning and at the end of each daytime emersion period. Thus, in the field, several samplings were carried out that have shown this particular pattern (see Guarini *et al*. 2000a,b and this chapter). This is an important result of this model that allowed us to define accurately the relevant temporal scale at which to observe the system. In return, the field observations confirmed the relevance of the conceptual basis of the model formulation.

Three modelling hypotheses were tested. The first hypothesis did not include any resuspension of the biofilm and the production period (and the presence of the biofilm at the mud surface) coincided with the daytime emersion period. The microphytobenthic community was synchronized with the tidal and the light dark cycles, and anticipated any refloodling in this scheme. However, the determinism of the downward migration is not well-known. Because of the variability in the tidal oscillation (due to the variability of the meteorological conditions of pressure and wind), the downward migration, in this scheme, has to be induced by an external forcing factor. The stimulus must come from the hydrodynamic processes.

The second modelling hypothesis included resuspension provoked by the variability in the tidal oscillation and assuming that the microphytobenthic community cannot anticipate an early refloodling. The production periods still coincided with the daytime emersion periods. Episodic resuspensions appeared like local disturbances

that deviated the biomass from its trajectory. The dynamics for the first two different modelling hypotheses converged to a unique cyclic equilibrium that was unconditionally stable. The recovery-time (*i.e.* the time necessary to reach values close to the asymptotic steady state from an initial condition $B_0 \geq S_{max}$) can be calculated. The approximate solution of the model was described by the series:

$$B_{n+1} = aB_n + b$$

which is also:

$$B_n = aB_{n-1} + b$$

And which can be developed as:

$$B_n - b(a^0+a^1+\ldots+a^{n-1}) = a^nB_0$$

If B_n is considered as the value close to the approximate solution B^*, $B_n=yB^*=yb/(1-a)$, where $y \in]0, 1[$. Practically, y is close to 1. $B^*(y-1) + a^nB^* = a^nB_0$ and then:

$$a^n = \frac{B^*(1-y)}{B^* - B_0}$$

or, after transformation :

$$n = \frac{\ln(B^*(1-y)/(B^* - B_0))}{\ln(a)}$$

with $\ln(a) = -(mT)$. n is to the number of sequences necessary to reach the value yB^*. The formulation of the recovery time, t_R, is:

$$t_R = \frac{\ln(B^*(1-y)/(B^* - B_0))}{-m}$$

The recovery time mainly depends on the relative difference between the initial condition B_0 and the steady state value B*. It will also increase when the value of y get closer to 1. The recovery time depends on the value of the loss rate m (and depends on its units): the smaller the loss rate, the longer the recovery time. The recovery time does not depend on either the production rate, or on the saturation value S_{max}. According to the order of magnitude of the parameters, the estimated recovery time to reach 95% of the steady state is about two weeks long, and decreases as B_0 approaches B^* (Figure 14).

The third modelling hypothesis was significantly different from the two previous ones. It assumed that the microalgal biomass is regulated by the community itself according to the following principle: when it reached a critical biomass, which depends locally on the saturation value at the mud surface and the duration of the daytime emersion period, the biofilm was resuspended into the water column. The

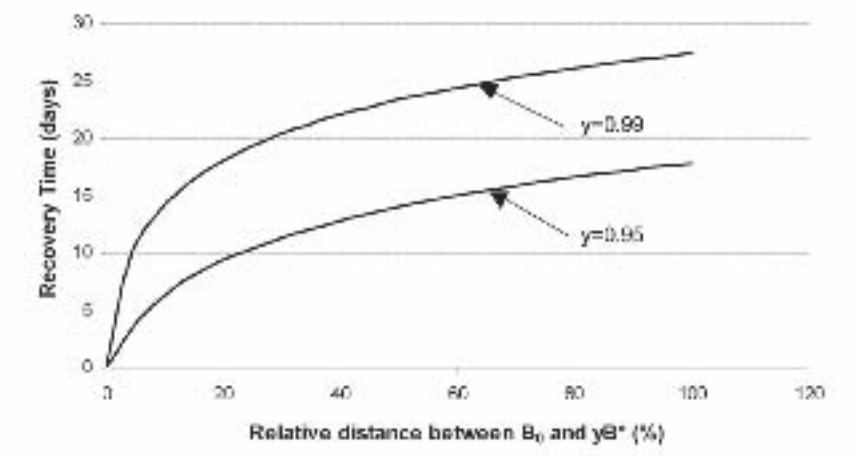

Figure 14. Recovery time as a function of the distance between the initial condition and the steady-state condition of the chlorophyll a concentration for case A (Figures 4 and 12) which assumed that no resuspension of the microphytobenthos occurred.

dynamic was allowed to converge to several steady states according to the relative value of the parameters describing the production and the losses (by grazing or stress-induced mortality). Steady state values around the critical biomass were not unique and depended strongly on the initial condition. They were nevertheless contained in the interval: $[B_c\text{-}S_{max}; B_c+S_{max}]$. If the mortality became too high and was not compensated by production, the biomass decreased down to zero. The system is conditionally persistent. Recovery times were estimated numerically using typical orders of magnitude of the parameters and were about as fast as the recovery times calculated for the two previous modelling hypotheses (about 15 days long).

Loss processes, grazing, stress-induced mortality and resuspension

The three modelling hypotheses that were tested were all based on the same concept of a biofilm that ensures production, and quantifying the variability of the primary production rate was crucial. The resuspension of the microphytobenthic biomass under standard conditions (without sediment erosion) depended on the presence of the biofilm at the moment of reflooding during daytime. Each of the three model hypotheses become increasingly complex in terms of the model structure and the resulting dynamics. First there was no resuspension (downward vertical migration prevents such an event to happen), secondly, resuspension could be induced by random variability in the synchronizers of the vertical migration, and finally that resuspension depended on the community itself through its deterministic property of biofilm renewal for a restricted number of times.

The loss rate included both stress-induced mortality and grazing. It was small and was represented by the simplest formulation: a linear function of the microphytobenthic

biomass. Loss processes were nevertheless very important in the determination of steady state, recovery time and conditions of resuspension of the biomass. The lack of knowledge about these processes of loss remains an important limitation on our ability to simulate and predict accurately the dynamics of the microalgal biomass in littoral ecosystems. Methods for estimating quantitatively the grazing and mortality fluxes and rates have to be found that can be extrapolated over the entire ecosystem. Inverse and network analysis methods, which are able to estimate fluxes in foodwebs where information is lacking, could be used to estimate loss rates (Vezina and Platt 1988).

How to choose between the three model hypotheses: field work approach

One way to determine which modelling structure best represents the dynamics of the microphytobenthic biomass, is to compare simulations with observations of the system. The main differences concern the resuspension process and the duration of the biofilm during the daytime emersion period. From the benthic point of view, it is technically difficult at this time to observe simultaneously and continuously both the biomass and the biofilm at the scale of the intertidal mudflats. In addition, the model is strongly sensitive to the parameter variability which generates strong uncertainties in the biomass estimates.

In contrast, from a pelagic point of view, significant resuspension should be characterized at high tide by a gradient of high biomass from the shore to the subtidal area and by the transport and dilution of biomass in subtidal areas at low tide. Therefore, the phytoplankton biomass was sampled in the water column of the Marennes-Oléron Bay. A sampling cruise was carried out in anticyclonic conditions (atmospheric pressure greater than 1015 mbar), with low wind velocities (lower than *ca.* 2.0 $m.s^{-1}$). The cruise took place at the end of March 2003 when mortality rate was low and production rate was high (Blanchard *et al*. 1997). At this time of the year, the phytoplankton bloom did not yet start. The sampling was performed at neap tide when the daytime emersion period preceding the submersion was short and, hence, according to our third hypothesis, when the probability of the presence of the biofilm at the reflood was the highest. Finally, this sampling cruise was realized after a long period (greater than a month) of stable meteorological conditionsso as to be close to steady state conditions. The cruise was designed to sample a large area in a minimum amount of time; the chlorophyll *a* concentration and the turbidity were recorded along the route of the ship using a continuous multi-parameter station. Two consecutive sampling plans were realized, at high tide occurring at noon, and at low tide occurring *ca.* 6 hours later. Full details of this sampling are provided in Guarini *et al*. (submitted).

The results of the sampling (Figure 15) showed a gradient of biomass at high tide, with a maximum concentration greater than 12 (µg Chl *a*).l^{-1}. The suspended matter concentration values were lower than 100 $mg.l^{-1}$. Assuming that the microphytobenthic biomass is diluted in the first centimetre of the mud, and considering an average value of 100 $mg.m^{-2}$ of chlorophyll *a* in the first centimetre of the mud (Guarini *et al*. 1998), associated with an average dry sediment density equal to 16.10^6 $g.m^{-2}.cm^{-1}$,

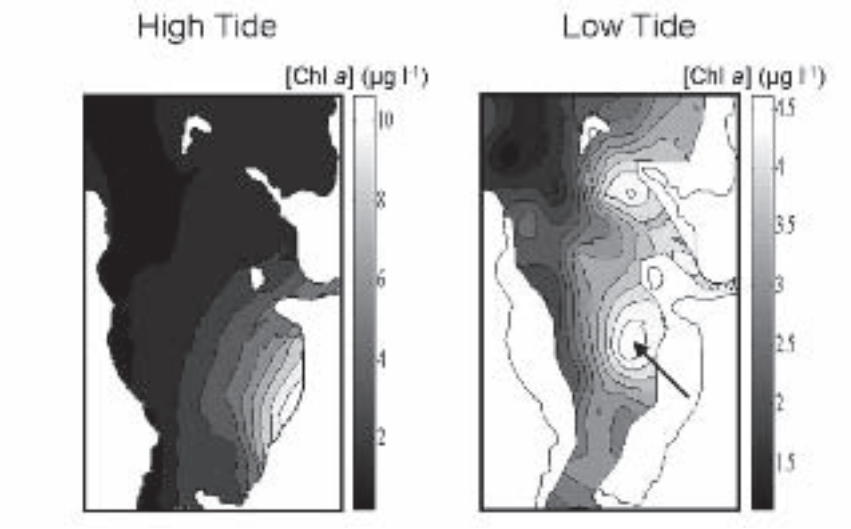

Figure 15. Spatial distribution of the phytoplankton biomass in terms of chlorophyll a concentration in the water of the Marennes-Oléron Bay, at the end of March 2003. The gradient of chlorophyll a concentration at high tide, followed by the advection-dispersion induced transport and the dilution at low tide of chlorophyll a concentration were evidence for the resuspension and export of the microphytobenthic biomass in the Marennes-Oléron Bay.

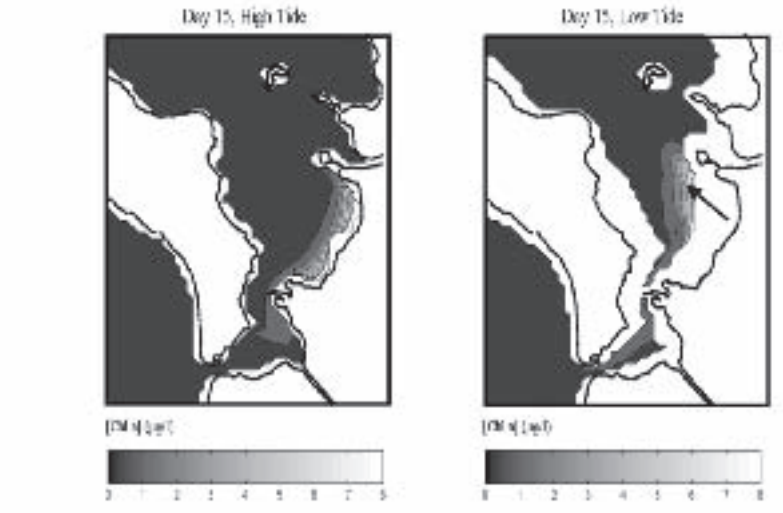

Figure 16. Simulation of the transport of the microphytobenthos in the Marennes-Oléron Bay. After 15 days, the results of the resuspension and transport of the microphytobenthos are consistent with the observed patterns (Figure 15).

the suspended matter concentration in *ca.* 1 m water column should have been equal to *ca.* 2.0 $g.l^{-1}$. This observation is strong evidence for the resuspension of the biomass without significant accompanying sediment erosion and the biofilm is the only structure that concentrates enough biomass to create a peak of resuspension at 12 µg Chl *a*. m^{-2}. At the following low tide, the resuspended biomass was observed to be transported in the central channel, at the northern part of the mudflat where it was diluted into deeper water. The chlorophyll *a* concentration decreased to 6 µg Chl $a.l^{-1}$. These patterns are consistent with the numerical modelling of the resuspension and transport of the biomass using the third hypothesis (summarized by the regulation of the population, Figure 16). Meteorological conditions were highly favourable to an increase of microphytobenthic biomass on the mudflat, but were not such that an early return of the tidal waters would be provoked. Therefore, the process of biofilm resuspension is self-regulated by the biomass and implied an absence of downward migration because the total biomass is greater than the critical biomass ($B_c = S_{max}(T_E/\tau_S)$). In addition, the resuspension of the biofilm may occurs without an associated sedimentary component. This hypothesis that biofilm resuspension occurs without sediment erosion, provides a reasonable and consistent explanation for the export of the microphytobenthic biomass from coastal semi-enclosed ecosystems that are usually considered as zones of net deposition.

Comparison between the dynamics of microphytobenthos and phytoplankton

The dynamics of the microphytobenthos can be characterized by a constant adjustment to steady state conditions that govern the seasonal trends. As a consequence, the within year variability is not very strong and depends more on meteorological conditions, which vary between years. Moreover, local conditions predominate since no spatial processes (passive or active transport) seem to influence the local dynamics. This is very different from the dynamics of the phytoplankton that is entirely governed by blooms, which can be seen as transitory phases, and stop when production nutrients become limited (Cloern 1996). Changes in limitation conditions often induce a succession of communities. Spatial processes of passive water mass transport control overall phytoplankton bloom dynamics (Lucas *et al*. 2000a,b).

In contrast, microphytobenthic production is mostly regulated by the space available at the surface of the mud. The mud surface is usually completely saturated during all or part of the daytime emersion period. Microphytobenthic production is also regulated by mud surface temperature that can vary quickly and widely during emersion periods. Light variations have a minimal impact, since most of the time light levels on the mudflat are saturating for photosynthetic activity (Guarini *et al*. 2002). For phytoplankton, light availability in fact, fluctuates strongly and completely controls production (specially in turbid waters), while temperature variations are small. Losses by stress-induced mortality and grazing, which are slow processes, influence the seasonal pattern of the microphytobenthos dynamics, while they do not have a strong impact of the phytoplankton dynamics during bloom events.

The net production of the microphytobenthos inhabiting intertidal mudflats was estimated in the Marennes-Oléron Bay by using the orders of magnitude which correspond to each parameter, and by considering an average value for the C: Chl *a* ratio equal to 40 (de Jonge 1980). The typical value of the net production is equal to 1 $gC.m^{-2}.day^{-1}$. This value is, in average, 4 times greater than the corresponding phytoplankton production in the bay (Raillard and Menesguen 1994). The microphytobenthic compartment is extremely productive, and has a strong potential for exportation to either the benthic foodwebs or to the water column through hydrodynamic resuspension.

Furthermore, our study pointed out that the resuspended microphytobenthos contributes to the biomass of the phytoplankton community. Resuspension may occurs on a daily basis; the microphytobenthic contribution varies in space and time, but is always significant at the scale of the ecosystem. Therefore, the comparison between the dynamics of the phytoplankton and microphytobenthos should be considered carefully, and should be replaced eventually by an integrated approach of the dynamics of benthic and pelagic microalgal biomasses in ETSELE.

Conclusions

The goal of this modelling study was to propose a consistent representation of the dynamics of the microphytobenthos inhabiting wide bare intertidal mudflats. This model was based on concepts that integrate the present knowledge. It nevertheless does not include all the concepts that were developed by many authors working on this topics, because some simplifications had to be made. For example, the species composition was not taking into account, because the species diversity is low, because no real pattern of succession was observed generally and the number of state variables would be too large, preventing any study of general mathematical properties. The model was designed to represent the dynamics of the microphytobenthos at the level of the ecosystem. Therefore, the small scale variability was filtered out. Finally a consistent representation has to be made, and controversial results could not be taken into account. For example, the presence of a biofilm, and a strong discontinuity at the mud surface could not be reconciled with the notion of a vertical profile of biomass and production.

The resulting model is one of the very few attempts to quantify specifically the dynamics of this compartment (see Blackford 2002 for subtidal areas). This contrasts with phytoplankton studies for which parts of theory already exist for many ecosystems: open ocean (Sverdrup, 1938), coastal ocean and shallow water ecosystems (Cloern 1996). This lack of coherent and consistent assessment strategies can be explained by a much shorter history of studying subtidal and intertidal mudflats, and by the enormous practical and technical difficulties in sampling mudflat systems. The most important problem currently is the lack of accurate measurements of the primary production under field conditions (Currin *et al*. 1996; Underwood and Kromkamp 2000). Estimates made on extracted microalgae need to be examined carefully, in order to decide if they were representative of *in situ* production, and if

the method of microphytobenthos extraction does not select preferentially some species of the community. The model discussed here does not solve these problems, but it does provide an integrated theoretical framework that can be tested and be used to determine experimental strategies about the microphytobenthos.

The model presented and discussed here is based on concepts and methods that originated with studies of the microphytobenthos, and were not based on the pelagic system of microalgal primary production. Intertidal benthic microalgae undergo fast changes due to their periodic alternation between air and water exposures. The physical environment of the microphytobenthos is not comparable to the physical conditions present in a well-mixed water column, and secondly, the strategies of the respective communities for production are also completely different. For example, the microphytobenthos community growth is due to vertical migration cycles toward the mud surface and the hourly changes in light irradiance and temperature that control the photosynthetic activity of the cells present at the mud surface during a daytime emersion period. Losses of the microphytobenthic biomass are not only through benthic grazing, but also plausibly from the resuspension of the biomass when it is swept away from the mud surface during each submersion period.

The 3 main features of the model are as follows:

1. The cycle of the vertical migration of the microalgae. The process is fast and was density-dependant in the model, but it was only partially described and the cell behaviour must be separated from the integrated result observed at the level of the community.
2. The creation of the biofilm at the mud surface during daytime emersion periods. The biofilm as a functional structure ensures the photosynthesis (controlled by light and mostly temperature) and hence the production of new biomass for the community. The biofilm must be better characterized in terms of accurate statistical estimates for both the number of cells and the biomass per unit of area.
3. A discrete 2-compartments structure. The biomass is concentrated at the mud surface (in the biofilm), and the remaining biomass is diluted in the first centimetre of the mud, with exchanges (through vertical migration) between each compartment.

The model provides a basis for describing the dynamics of the microphytobenthos that inhabits intertidal mudflats. On one hand, the model can incorporate many other processes as they are shown to be relevant in the regulation of the community at the level of the ecosystem. For example, nutrient availability and control on the production were not taken into account, but could be important if both the use of nutrient pools by microalgae and the fluxes of nutrients in the sediment are described. On the other hand, the model suggests that in order to understand completely the dynamics of the microphytobenthos in European-type semi-enclosed littoral ecosystems, it will be necessary to develop an integrated approach for the total microalgal biomass (benthic plus pelagic), an approach which will need to take into account explicitly exchanges of biomass between the benthic and pelagic compartments. This is one of the major challenges in littoral ecology, especially to quantify the contribution of the microphytobenthos in the carbon cycle and budget of coastal ecosystems.

References

ADMIRAAL, W. 1984. The ecology of estuarine sediment-inhabiting diatoms. In: Progress in Physiological Research, Round F.E, Chapman D.J. (ed.), Vol. 3. Bristol: Biopress Ltd. 269-322.

BLACKFORD, J.C. 2002. The Influence of Microphytobenthos on the Northern Adriatic Ecosystem: a Modelling Study. Estuar. Coast. and Shelf Sci. **55**: 109-123.

BLANCHARD, G.F., J.M. GUARINI, P. RICHARD and PH. GROS. 1997. Seasonal effect on the relationship between the photosynthetic capacity of intertidal microphytobenthos and short-term temperature changes. J. Phycol. **33**: 723-728.

BLANCHARD, G.F., J.M. GUARINI, C. DANG and P. RICHARD. Characterizing and quantifying photoinhibition in intertidal microphytobenthos. Submitted to J. Phycol.

BLANCHARD, G.F and V. CARIOU-LE GALL. 1994. Photosynthetic characteristics of microphytobenthos in Marennes-Oleron Bay, France: Preliminary results. J. Exp. Mar. Biol. Ecol. **182**: 1-14.

CLOERN, J.E. 1996. Phytoplankton bloom dynamics in coastal ecosystems: a review with some general lessons from sustained investigation of San Francisco Bay, California. Rev. Geophys. **34**: 127-168.

COUCH, C.A. 1989. Carbon and nitrogen stable isotopes of meiobenthos and their food resources. Estuar. Coast. Shelf Sci. **28**: 433-41.

CURRIN, C.A., L. LEVIN and T. SINICROPE. 1996. Factors affecting intertidal benthic microalgal production in East and West Coast marsh habitats. Conference: 24th. Ann. Benthic Ecology Meeting, Columbia, SC (USA), 7-10 Mar 1996. page 94.

DEMERS, S., J.C. THERRIAULT, E. BOURGET and A. BAH. 1987. Resuspension in the shallow sublittoral zone of a macrotidal estuarine environment: wind influence. Limnol. Oceanogr. **32**: 327-339.

FROUIN, R., D.W. LINGNER, C. GAUTIER, K.S. BAKER and R.C. SMITH. 1989. A simple analytical formula to compute clear sky total and photosynthetically available solar irradiance at the ocean surface. J. Geophys. Res. **94**: 9731-9742.

GUARINI, J.M. 1998. Modélisation de la dynamique du microphytobenthos des vasières intertidales du bassin de Marennes-Oléron. Effet des synchroniseurs physiques sur la régulation de la production. Thèse de Doctorat – Océanologie - Université de Paris 6. 177pp.

GUARINI, J.M., G.F. BLANCHARD, C. BACHER, PH. GROS, P. RIERA, P. RICHARD, D. GOULEAU, R. GALOIS, J. PROU and P.G. SAURIAU. 1998. Dynamics of spatial patterns of microphytobenthic biomass: inferences from a geostatistical analysis of two comprehensive surveys in Marennes-Oléron Bay (France): results from a geostatistical approach. Mar. Ecol. Prog. Ser. **166**: 131-141.

GUARINI, J.M., G.F. BLANCHARD, PH. GROS and S.J. HARRISON. 1997. Modelling the mud surface temperature on intertidal flats to investigate the spatio-temporal dynamics of the benthic micro-algal photosynthetic capacity. Mar. Ecol. Prog. Ser. **153**: 25-36.

GUARINI, J.M., G.F. BLANCHARD, PH. GROS, D. GOULEAU and C. BACHER. 2000a. Dynamic model of the short-term variability of microphytobenthic biomass on temperate intertidal mudflat. Mar. Ecol. Prog. Ser. **195**: 291-303.

GUARINI, J.M., G.F. BLANCHARD and PH. GROS. 2000b. Quantification of the microphytobenthic primary production in European intertidal mudflats: a modelling approach. Cont. Shelf Res. **20**: 1771-1788.

HARRISON S.J. and A.P. PHIZACKLEA. 1987. Vertical temperature gradients in muddy intertidal sediments in the Forth estuary, Scotland. Limnol. Oceanogr. **32**: 954-63.

HAY S.I., T.C. MAITLAND and D.M. PATERSON. 1993. The speed of diatom migration through natural and artificial substrata. Diatom Res. **8**: 371-384.

JASSBY, A.D. and T. PLATT. 1976. Mathematical formulation of the relationship between photosynthesis and light for phytoplankton. Limnol. Oceanogr. **21**: 540-547.

JONGE, V.N. DE. 1980. Fluctuations in the organic carbon to chlorophyll a ratios for estuarine benthic diatoms populations. Mar. Ecol. Prog. Ser. **2**: 345-53.

JONGE, V.N. DE and J.E.E. VAN BEUSEKOM. 1992. Contribution of resuspended microphytobenthos to total phytoplankton in the Ems Estuary and its possible role for grazers. Neth. J. Sea. Res. **30**: 91-105.

JONGE, V.N. DE, and J.E.E. VAN BEUSEKOM. 1995. Wind- and tide-induced resuspension of sediment and microphytobenthos from tidal flats ins the Ems estuary. Limnol. Oceanogr. **40**: 766-778.

LE HIR, P., W. ROBERTS, O. CAZAILLET, M. CHRISTIE, P. BASSOULLET and C. BACHER. 2000. Characterisation of intertidal flat hydrodynamics. Cont. Shelf Res. **20**: 1433-1459.

LEGENDRE, L. 1981. Hydrodynamic control of marine phytoplankton production: the paradox of stability. In Ecohydrodynamics. J.C.J. Nihoul ed. Elsevier Oceanography Series, 32. Elsevier, Amsterdam, Oxford, New York., 191-208.

LONG, S.P. and C.F. MASON. 1983. Saltmarsh ecology. Blackie, Glasgow. 168 pp.

LUCAS, L., J.E. CLOERN, J.R. KOSEFF, S.G. MONISMITH and J.K. THOMPSON. 1998. Does the Sverdrup critical depth model explain bloom dynamics in estuaries. J. Mar. Res. **56**: 375-415.
LUCAS, C.H., C. BANHAM, and P.M. HOLLIGAN. 2001. Benthic-pelagic exchange of microalgae at a tidal flat. 2. Taxonomic analysis. Mar. Ecol. Prog. Ser. **212**: 39-52.
LUCAS, L., J.R. KOSEFF, J.E. CLOERN, S.G. MONISMITH and J.K. THOMPSON. 1999a. Processes governing phytoplankton blooms in estuaries. I: The local production-loss balance. Mar. Ecol. Prog. Ser. **187**: 1-15.
LUCAS, L., J.R. KOSEFF, S.G. MONISMITH, J.E. CLOERN and J.K. THOMPSON. 1999b. Processes governing phytoplankton blooms in estuaries. II: The role of horizontal transport. Mar. Ecol. Prog. Ser. **187**: 17-30.
MARRA, J. 1978. Phytoplankton Photosynthesis response to vertical movement in the mixed layer. Mar. Biol. **46**: 203-208.
MCDONALD, E.T. and R.T. CHENG. 1997. A numerical model of sediment transport applied to San Francisco Bay, California. J. Mar. Environ. Eng. **4**: 1-41.
MCLUSKY, D.S. 1989. The estuarine ecosystem. 2nd edition. New York: Chapman & Hall. 215 pp.
MILLER, D.R. 1974. Sensitivity analysis and validation of simulation models. J. theor. Biol. **48**: 345-360.
PALMER, J.D. and F.E. ROUND. 1965. Persistent, vertical migration rhytms in benthic microflora. I. The effect of light and temperature on the rhytmic behaviour of Euglena obtusata. J. Mar Biol. Ass. U. K. **45**: 567-582.
PALMER, J.D. and F.E. ROUND. 1967. Persistent, vertical migration rhytms in benthic microflora. VI. The The tidal and diurnal nature of the rhythm in the diatom Hantzschia virgata. Biol. Bull. **132**: 44-55.
PATERSON, D.M. 1989. Short-term changes in the erodibility of intertidal cohesive sediments related to the migratory behavior of epipelic diatoms. Limnol. Oceanogr. **34**: 223-234.
PATERSON, D.M., R. DOERFFER, J. KROMKAMP, G. MORGAN and W. GIESKE, 1998. Assessing the biological et physical dynamics of intertidal sediment ecosystems. A remote sensing approach (project BIOPTIS). Barthel, K.G. (ed.), Barth, H. (ed.), Bohle-Carbonell, M. (ed.), Fragakis, C. (ed.), Lipiatou, E. (ed.), Martin, P. (ed.), Ollier, G. (ed.). Third european MArine Science et Technology Conference,Lisbon (Portugal), 23-27 May 1998. pages 377-390.
PINCKNEY, J.L. and R.G. ZINGMARK. 1991. Effects of tidal stage and sun angles on intertidal benthic microalgal productivity. Mar. Ecol. Prog. Ser. **76**: 81-89.
PINCKNEY, J.L. and R.G. ZINGMARK. 1993. Modelling the annual production of intertidal benthic microalgae in estuarine ecosystems. J. Phycol. **29**: 3 96-407.
PRITCHARD, D.W. 1967. Observations of circulation in coastal plain estuaries. In Estuaries (G.H. Lauff, ed.) AAAS, Washington DC. **83**: 37-44.
RAILLARD, O. and A. MENESGUEN. 1994. An ecosystem box model for estimating the carrying capacity of a macrotidal shellfish system. Mar. Ecol. Prog. Ser. **115**: 117-130.
SABUROVA M.A., I.G. POLIKARPOV and I.V. BURKOVSKY. 1995. Spatial structure of an intertidal sandflat microphytobenthic community as related to different spatial scales. Mar. Ecol. Prog. Ser. **129**: 229-239.
SCHELSKE, C.L. and E.P. ODUM. 1962. Mechanisms maintaining high productivity in Geogia estuaries. Proc. Gulf Carrib. Fish Inst. **14**: 75-80.
SERÔDIO J., J.M. DA SILVA and F. CATARINO. 1997. Non destructive tracing of migratory rhythms of intertidal benthic microalgae using in vivo chlorophyll a fluorescence. J. Phycol. **33**: 542-553.
SERÔDIO, J. and F. CATARINO. 2000. Modelling the primary productivity of intertidal microphytobenthos: Time scales of variability et effects of migratory rhythms. Mar. Ecol. Prog. Ser. **192**: 13-30.
SEURONT, L. and N. SPILMONT. 2002. Self Organized criticality in intertidal microphytobenthos patch patterns. Physica A: statistical mechanics and its applications. **313**: 513-539.
SHAFFER, G.P. and M.J. SULLIVAN. 1988. Water column productivity attribuatable to displaced benthic diatoms in well-mixed shallow estuaries. J. Phycol. **24**: 132-140.
SVERDRUP, H.U. 1953. On conditions for the vernal blooming of phytoplankton. Journal du Conseil International pour l'Exploitation de la Mer. **18**: 287-295.
UNDERWOOD, G.J.C. and J. KROMKAMP. 2000. Primary production by phytoplankton and microphytoplankton in estuaries. In: Nedwell DB, Raffaelli DG (eds) Estuaries. Advances in Ecological Research, Academic Press. Pages 93-153.
VAN BOXEL, J.H. 1986. Heat balance investigations in tidal areas. PhD Thesis, University of Amsterdam, Netherland : 137 p.
VÉZINA, A.F. and T. PLATT. 1988. Food web dynamics in the ocean. I best estimates using inverse methods. Mar. Ecol. Prog. Ser. **42**: 269-287.
WALKER, H.J. and J. MOSSA. 1982. Effects of artificial structures on coastal lagoon processes and forms. Oceanol. Acta. **5**: 191-198.
WETZEL, R.L. and Y.-S. SIN. 1998. Ecosystem Process Models: Applications to Wetland Systems. Ocean. Res. **2**: 189-197.